



Universidade de Aveiro

2022

**Alexandre Braga
Barbosa**

**Techniques for Evaluation and
Minimization of Coupling in Antenna Array
Systems**

**Técnicas para Avaliação e Minimização de
Acoplamento em Sistemas de agregados
de antenas**



Universidade de Aveiro

2022

**Alexandre Braga
Barbosa**

**Techniques for Evaluation and Minimization of
Coupling in Antenna Array Systems**

Dissertação apresentada à Universidade de Aveiro para cumprimento dos requisitos necessários à obtenção do grau de Mestre em Engenharia Eletrónica e Telecomunicações, realizada sob a orientação científica do Doutor João Nuno Pimentel da Silva Matos, professor associado da Universidade de Aveiro, e do Doutor Tiago Miguel Valente Varum, investigador do Instituto de Telecomunicações.

O júri / The jury

Presidente / President

Professor Doutor Telmo Reis Cunha
Professor Associado, Universidade de Aveiro

Vogais / Committee

Professor Doutor Rafael Ferreira da Silva Caldeirinha
Professor Coordenador C/Agregação, Instituto Politécnico de Leiria

Professor Doutor João Nuno Pimentel da Silva Matos
Professor Associado, Universidade de Aveiro (orientador)

**Agradecimentos/
Acknowledgments**

Inicialmente gostaria de agradecer ao meu pai Adelino Alberto Barbosa, à minha mãe Eva Braga e ao meu irmão Filipe Braga Barbosa por sempre me ajudarem no meu percurso, tanto académico como pessoal, tornado assim a pessoa que sou hoje num homem melhor a vários níveis.

Em segundo lugar, quero dar um agradecimento ao orientador professor João Nuno Matos e ao coorientador Tiago Miguel Varum, por toda a disponibilidade e ajuda, desde o esclarecimento de dúvidas e problemas até à orientação do melhor caminho a seguir em cada etapa desta dissertação.

Gostaria também de agradecer à Universidade de Aveiro, Departamento de Eletrónica Telecomunicações e Informática e ao Instituto de Telecomunicações, que me acolheram nos últimos cinco anos.

Por fim quero dar um agradecimento especial a todos os amigos, colegas e pessoas que se cruzaram comigo nos últimos cinco anos.

Palavras-chave

5G, Comunicações de satélites, Arrays faseados, Beamforming.

Resumo

A evolução dos sistemas MIMO modernos tem levado estes a operar cada vez mais em frequências em torno de ondas milimétricas na procura de maiores larguras de banda, assim como na procura por maiores ganhos das antenas, e capacidade de *beamforming* ou filtragem espacial. Para isso, essa elevada densidade de antenas num curto espaço alerta para o aparecimento de fenómenos indesejáveis, como são o acoplamento mútuo entre os elementos, que degradam a performance destes sistemas, tornando-se necessário encontrar técnicas para minimizar esse efeito.

Nesta dissertação esta problemática foi analisada, e são apresentadas soluções que possibilitam a redução deste efeito negativo em agregados de antenas. Nesse sentido, foram desenvolvidas duas estruturas impressas, com propriedades associadas aos metamateriais, propriedades estas que têm ganho bastante relevo nas últimas décadas na melhoria de sistemas MIMO em vários aspetos, uma em forma de U e outra com uma variação resultante da junção de dois anéis.

Posteriormente foi feito um estudo comparativo em simulação do impacto das duas estruturas em diferentes situações (estando as antenas patch calibradas para 8.4GHz), sendo finalmente comparados os resultados obtidos por simulação com as medidas obtidas em laboratório para arrays de 4 elementos com e sem os metamateriais em forma de U e analisou-se o efeito destas estruturas no agregado.

Keywords

5G, Satellite Communications, Phased Arrays, Beamforming.

Abstract

The evolution of modern MIMO systems has led them to increasingly operate at frequencies around millimeter waves in the search for greater bandwidth, as well as in the search for greater antenna gains, and *beamforming* or spatial filtering capabilities. For this, the high density of antennas in a short space alerts to the appearance of undesirable phenomena, such as the mutual coupling between the elements, which degrade the performance of these systems, making it necessary to find techniques to minimize this effect.

In this dissertation, this problem was analyzed, and solutions are presented that allow the reduction of this negative effect in antenna aggregates. In this sense, two printed structures were developed, with properties associated with metamaterials, one in the shape of a U and the other with a variation resulting from the joining of two rings.

Subsequently, a comparative study was carried out in simulation of the impact of the two structures in different situations (with patch antennas calibrated to 8.4GHz), finally the results obtained by simulation were compared with the measurements obtained in the laboratory for arrays of 4 elements with and without the U-shaped metamaterials, and the effect of these structures on the array was analysed.

Contents

List of Figures	III
List of tables	V
List of acronyms	VII
1. Introduction	1
1.1 Context and Motivation	1
1.2 Objectives and methodology of the dissertation	3
1.3 Dissertation Structure	4
2. Overview on antennas, antenna array and coupling	5
2.1 Microstrip antennas.....	5
2.2 Antenna parameters	6
2.3 Design of a single antenna with recessed alimentation	7
2.3.1 Width and length	7
2.3.2 Y_0 and power line width of characteristic impedance $Z_0 = 50\Omega$	8
2.3.3 Design of a single antenna with coaxial alimentation.....	9
2.4 Coupling paths for the antenna elements	10
2.4.1 Transmission mode.....	10
2.4.2 Receiving mode	11
2.5 Types and other consequences of coupling	11
2.6 Scan blindness.....	13
2.7 Effects of coupling using the RWG method	14
2.6 State of art-Previous techniques to reduce the coupling.....	15
2.6.1 EBG (Electromagnetic band-gap)	15
2.6.2 DGS (Defected Ground Structure)	15
2.6.3 Meander line	17
2.6.4 Metamaterial.....	18
3. Metamaterials	21
3.1 Motivation to use metamaterials.....	21
3.2 Metamaterials.....	21
3.2.1 Properties of metamaterials	21
3.2.2 Design of metamaterials	24
4. Simulated Results	29
4.1 Design and simulation of the metamaterials	29
4.2 Simulated results	34
4.2.1 U Shape metamaterial in an array with coaxial feed	34
4.2.2 Double ring metamaterial in an array with coaxial feed	37
4.2.3 U Shape metamaterial in an array with recessed feed	39
5. Prototypes and measured results	41
5.1 Design and comparison of the coupling.....	41
5.2 Comparison of other parameters apart from coupling	47

6. Conclusions and future work	51
6.1 Conclusions.....	51
6.2 Future work.....	51
References	53

List of Figures

FIGURE 1.1-MIMO SYSTEM[1]	1
FIGURE 1.2-BEAMFORMING SYSTEM[1]	2
FIGURE 1.3-BEAMFORMING ON ANTENNA ARRAY[2]	2
FIGURE 1.4-ANTENNAS RADIATING ON A SPECIFIC ANGLE[2]	3
FIGURE 2.1-ANTENNA WITH A RECESSED MICROSTRIP-LINE FEED.....	6
FIGURE 2.2-EXEMPLE OF AN ANTENNA ARRAY WITH TWO ELEMENTS	6
FIGURE 2.3-NORMALIZED INPUT RESISTANCE[7]	9
FIGURE 2.4-ANTENNA BEING FEED BY THE COAXIAL TECHNIQUE	9
FIGURE 2.5-COUPLING ON THE TRANSMISSION MODE[7]	10
FIGURE 2.6-COUPLING ON THE RECEIVING MODE[7].....	11
FIGURE 2.7-TYPES OF WAVES PROPAGATING ON THE PATCHES THAT CAUSES COUPLING[11]	12
FIGURE 2.8-VARIATION OF THE INPUT REFLECTION COEFFICIENT WITH THE ANGLE[7]....	13
FIGURE 2.9-VARIANCE OF THE GAIN WITH THE ANGLE[7]	13
FIGURE 2.10-RWG METHOD ON AN ANTENNA ARRAY	14
FIGURE 2.11-EBG STRUCTURE.....	15
FIGURE 2.12-DGS STRUCTURE.....	15
FIGURE 2.13-CURRENT FLOWING THROUGH DGS, AND DGS SCHEMATIC	16
FIGURE 2.14-MEANDER LINE SCHEMATIC.....	17
FIGURE 2.15-CSRR SCHEMATIC.....	18
FIGURE 2.16-METAMATERIAL WITH A HILBERT DESIGN[20]	18
FIGURE 2.17-EFFECTS OF CURRENT ON THE STRUCTURES[19]	19
FIGURE 3.1-SCHEMATIC OF A NORMAL REFRACTION[23].....	22
FIGURE 3.2-SCHEMATIC OF A NEGATIVE REFRACTION[23]	22
FIGURE 3.3-ILLUSTRATIONS OF DIRECTIONS OF ELECTRIC FIELD, MAGNETIC FIELD, POYTING VECTOR AND WAVE VECTOR ON A RIGHT-HANDED MEDIUM[24].....	23
FIGURE 3.4-ILLUSTRATIONS OF DIRECTIONS OF ELECTRIC FIELD, MAGNETIC FIELD, POYTING VECTOR AND WAVE VECTOR ON A LEFT-HANDED MEDIUM[24].....	24
FIGURE 3.5-RE-ENTRANT CAVITY[26]	25
FIGURE 3.6-EQUIVALENT CIRCUITS OF DIFFERENT METAMATERIALS[26].....	26
FIGURE 3.7-EQUIVALENT CIRCUITS OF SRR AND CSRR[27].....	27
FIGURE 3.8-EXAMPLES OF DIFFERENT METAMATERIALS [27].....	28
FIGURE 4.1-2D PLAN AND EQUIVALENT RESONANT FREQUENCY OF THE VARIATION OF A U SHAPE METAMATERIAL.....	30
FIGURE 4.2-2D PLAN AN EQUIVALENT RESONANT FREQUENCY OF THE VARIATION OF A U SHAPE METAMATERIAL WITH AN X OF 1.2MM	30
FIGURE 4.3-2D PLAN AN EQUIVALENT RESONANT FREQUENCY OF THE VARIATION OF A U SHAPE METAMATERIAL WITH AN C OF 4.5MM.....	31
FIGURE 4.4-FLOQUET PORT MODE OF THE UNIT CELL	31
FIGURE 4.5-FLOW OF THE CURRENTS ON THE U-SHAPE METAMATERIAL ARMS.....	32

FIGURE 4.6-2D PLAN AND EQUIVALENT RESONANT FREQUENCY OF THE VARIATION OF A TWO RING METAMATERIAL	32
FIGURE 4.7-2D PLAN AND EQUIVALENT RESONANT FREQUENCY OF THE VARIATION OF A TWO RING METAMATERIAL WITH THE RINGS CLOSER.....	33
FIGURE 4.8-2D PLAN AND EQUIVALENT RESONANT FREQUENCY OF THE VARIATION OF A TWO RING METAMATERIAL WITH THE SIZE OF THE RINGS ENLARGED	33
FIGURE 4.9-FLOW OF THE CURRENTS ON THE DOUBLE RING METAMATERIAL ARMS	34
FIGURE 4.10-S ₂₁ WITH AND WITHOUT METAMATERIAL	34
FIGURE 4.11-TOTAL EFFICIENCY WITH AND WITHOUT METAMATERIAL	35
FIGURE 4.12 -DIAGRAMS OF RADIATION WITH AND WITHOUT THE METAMATERIAL	35
FIGURE 4.13-ECC AND DIVERSITY GAIN WITH AND WITHOUT METAMATERIAL.....	36
FIGURE 4.14-SURFACE CURRENTS (0 TO 3A/M) WITHOUT AND WITH THE METAMATERIAL	36
FIGURE 4.15-DIRECTION OF THE ADJACENT CURRENTS WITHOUT THE METAMATERIAL...	37
FIGURE 4.16-DIRECTION OF THE ADJACENT CURRENTS WITH THE METAMATERIAL	37
FIGURE 4.17-S ₂₁ WITH AND WITHOUT METAMATERIAL	38
FIGURE 4.18-TOTAL EFFICIENCY WITH AND WITHOUT METAMATERIAL	38
FIGURE 4.19-DIAGRAMS OF RADIATION WITH AND WITHOUT THE METAMATERIAL	39
FIGURE 4.20-ECC AND DIVERSITY GAIN WITH AND WITHOUT METAMATERIAL.....	39
FIGURE 4.21-S ₂₁ WITH AND WITHOUT METAMATERIAL	40
FIGURE 5.1-NUMBERING OF THE ANTENNA ELEMENTS.	42
FIGURE 5.2-S ₁₁ WITH AND WITHOUT METAMATERIAL	42
FIGURE 5.3-S ₂₁ AND S ₃₁ WITH AND WITHOUT METAMATERIAL.....	43
FIGURE 5.4-S ₄₁ WITH AND WITHOUT METAMATERIAL	43
FIGURE 5.5-METAMATERIAL PROTOTYPES FABRICATED.....	44
FIGURE 5.6-S ₁₁ , S ₂₁ , S ₃₁ AND S ₄₁ SIMULATED AND MEASURED WITH METAMATERIAL	45
FIGURE 5.7-S ₁₁ , S ₂₁ , S ₃₁ AND S ₄₁ MEASURED WITH AND WITHOUT METAMATERIAL....	46
FIGURE 5.8-TOTAL EFFICIENCY WITH AND WITHOUT METAMATERIAL	48
FIGURE 5.9-REALIZED GAIN WITH AND WITHOUT METAMATERIAL	48
FIGURE 5.10-ECC AND DIVERSITY GAIN WITH AND WITHOUT METAMATERIAL.....	49
FIGURE 5.11-DIAGRAMS OF RADIATION WITH AND WITHOUT THE METAMATERIAL	49

List of tables

TABLE 4.1-VALUES OF THE SQUARE METAMATERIAL PARAMETERS	30
TABLE 4.2-VALUES OF THE CIRCULAR METAMATERIAL PARAMETERS	32
TABLE 5.1-SIMULATED AND MEASURED VALUES OF THE ANTENNA ARRAY WITH AND WITHOUT METAMATERIAL	47

List of acronyms

CSRR:	Complementary Split Ring Resonator
CRR:	Complementary Ring Resonator
DGS:	Defected Ground Structure
DG:	Diversity Gain
EBG:	Electromagnetic band-gap
ECC:	Envelope Correlation Coefficient
FSS:	Frequency Selective Surface
MTM:	Magnetic metamaterials
MIMO:	Multiple input multiple output
MC:	Mutual coupling
SNG:	Single Negative Gaps
SRR:	Single Ring Resonator
LC:	Tuned Circuit
WG-MTM:	Waveguide Metamaterial
RWG:	Rao-Wilton-Glisson

1. Introduction

The first chapter will provide a brief introduction for this dissertation, explaining the motivation and its contextualization in the modern days.

1.1 Context and Motivation

The progress of wireless communications has increased, which leads for higher users demand for more and better consumption of information in their daily lives. New technologies were developed, moving to frequencies around millimetre waves in search of higher bandwidths to fulfil their needs and/or finding chunks of electromagnetic spectrum available to meet the needs of each application.

This progress in technologies and applications is what makes possible for users to do things that were never possible before, such as, downloading big files in minutes, watch streams at a higher resolution and play demanding video games in real time.[1]

Adaptive antenna systems and their beamforming capabilities are, in conjunction with MIMO (Multiple input multiple output) systems (figure 1.1), the most common advanced techniques used by these applications to suppress the demands of nowadays society technologies.

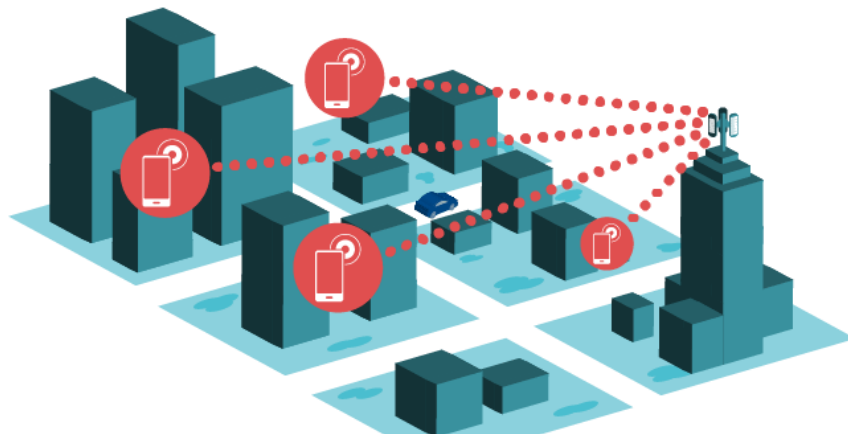


Figure 1.1-MIMO system[1]

In MIMO systems, there are a lot of elements radiating on a small space which allows multiple users to share the same network resources simultaneously, without major problems by increasing the network capacity and improving coverage (figure 1.2).



Figure 1.2-Beamforming system[1]

On the following example, all the elements of the antenna have the same frequency, spacing and phase, which results on a more powerful signal sent to the user (figure 1.3).

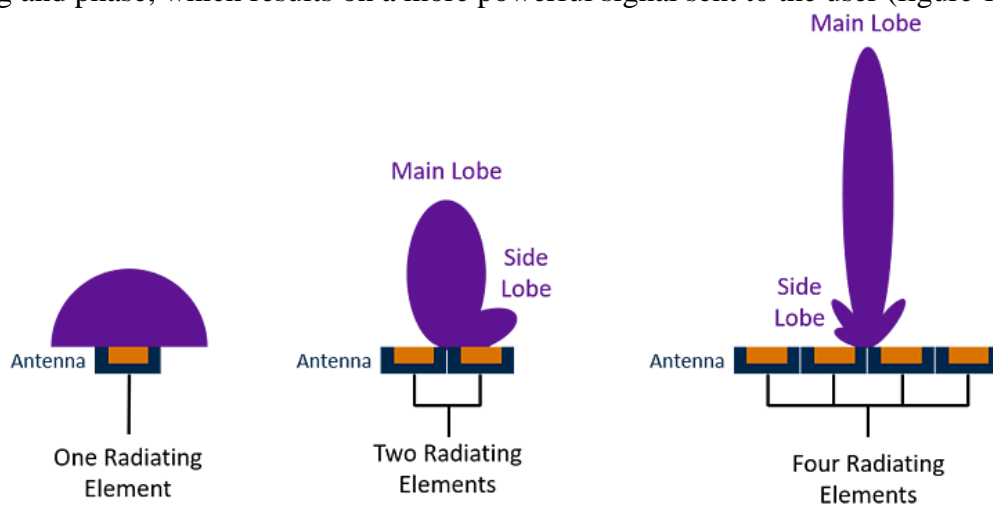


Figure 1.3-Beamforming on antenna array[2]

However, beamforming can be used along with MIMO technologies on different ways, by phasing out some elements in relation to others on the same antenna array, in order to send information to several users.

On the following example (figure 1.4) it's possible to see both techniques used together resulting on a more powerful signal to two users.

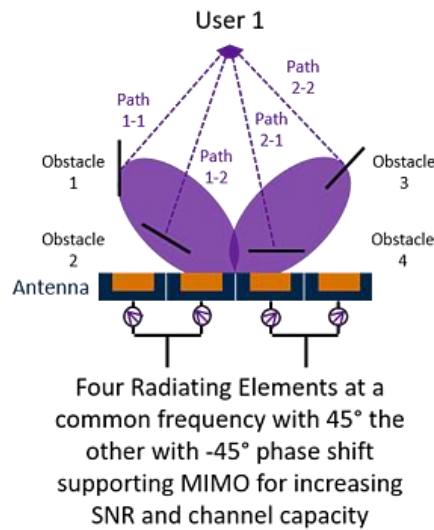


Figure 1.4-Antenas radiating on a specific angle[2]

In spite of that, more and more compact, and smaller arrays are wanted to be used in those modern technologies and, increasing these systems with dozens or hundreds of radiating elements, arranged in a reduced area to improve the signal powers, would lead to the appearance of several undesirable problems, such as excessive interference by a beamformed signal's side lobe and the coupling between elements, that is, the effect of the energy that is radiated by an antenna to his neighbouring antennas, and the way it affects the behaviour of his neighbouring antennas.

Considering all that was said before, it can be concluded that in modern times, it's important to create advanced systems which are small and compact, and also keeping in mind that their functionality and reliability will not compromise the performance of each other's.

1.2 Objectives and methodology of the dissertation

In this work, the objective involves the study of coupling between elements in an array of antennas, as well as the development of a technique that allow the MC (Mutual coupling) reduction, and, therefore, contribute to an improvement in the performance of adaptive antenna systems or MIMO.

To accomplish the understanding of this knowledge, it will be given insights into theoretical concepts of antennas, MC between the antennas, and the techniques and structures used to reduce the MC.

In the end, it will also be given a practical situation by simulating and manufacturing the proposed simulated prototypes which were based on the theoretical and simulated concepts.

1.3 Dissertation Structure

This dissertation is divided into six chapters, each of them addressing a different and relevant topic of it, as described below:

- **Chapter 1:** The opening chapter of this dissertation intends to introduce the motivations and objectives.
- **Chapter 2:** The second chapter goes in deep about the theoretical concepts behind antennas and electromagnetic interactions between the antenna elements in an array (mutual coupling). It also provides an overlook on previous techniques (state of art) to reduce the coupling of MIMO systems.
- **Chapter 3:** This chapter analyses with more profundity metamaterials, which are the foundation of the technique that will be used in this dissertation to reduce the mutual coupling between elements.
- **Chapter 4:** The fourth chapter describes the simulated process of the elements on CST, in specific the design and simulations of the metamaterials that were used to reduce the mutual coupling, the antenna arrays used, and the analysis of the results of the arrays with and without the metamaterial.
- **Chapter 5:** This chapter describes the measurement methods, results, and more analysis of the manufacture of some arrays analysed on the previous chapter.
- **Chapter 6:** In the close chapter are presented the conclusions of the work developed and suggestions for future work.

2. Overview on antennas, antenna array and coupling

This chapter aims to give the reader a better understanding of some concepts of this dissertation, as well as some work done on the main focus, coupling strategies to reduce mutual coupling between elements on an antenna array.

With this in mind, firstly microstrip antennas and some of its main parameters will be introduced.

Secondly, it will be discussed how coupling is created and transmitted from element to element, and how it damages the performance of the MIMO systems.

To conclude, a state-of-art review regarding techniques to reduce mutual coupling in MIMO arrays is shown to provide a brief insight into these technologies.

2.1 Microstrip antennas

A patch is a type of radio antenna that consists of a very thin metal plate (“patch”), placed on a bigger metal surface called a ground, with the separation between them made by a dielectric. These two metallic surfaces, together, form a resonant circuit with a length of about $\frac{\lambda}{2}$.

The versatility, its simplicity, its reduced size and cost, and its good adaptation to various types of surfaces and frequencies are advantages of this type of antenna.

Furthermore, its manufacturing simplicity using printed circuit, makes the use of this type of antennas appropriate for countless applications.

It must be borne in mind that this type of antenna entails some disadvantages compared to other types, namely the low transmission power, the low gain (the typical maximum gain is around 7 dB) and a narrow bandwidth.

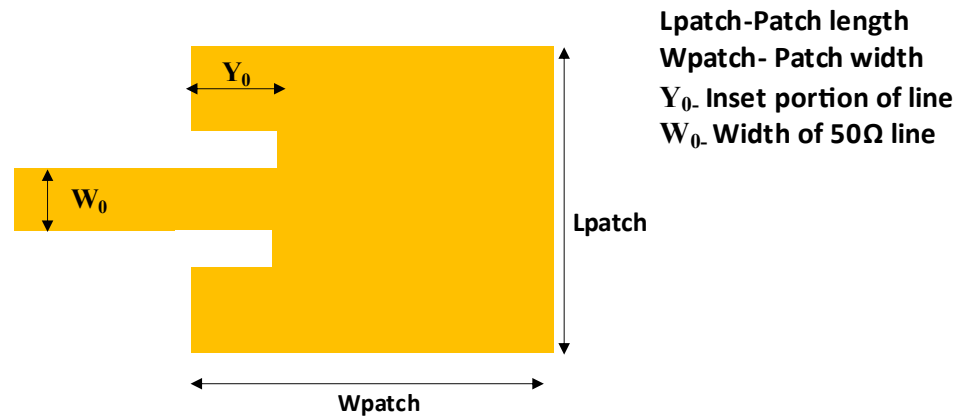


Figure 2.1-Antena with a recessed microstrip-line feed

Although having the disadvantages mentioned previously, several of these antennas can be placed together and form an antenna array with higher values of transmission power, directivity, and gain of the system without losing the other advantages mentioned before. On top of that, in an antenna array, the more elements it has, the stronger the signal of the main lobe will be.

Furthermore, all the advantages considered before can also be achieved by placing the elements of the array closed together. However, there is a sense of a downfall performance, because the closer they are to each other, the more MC between them it will be.

Even though a lot of applications use antennas with a recessed-line feed (figure 2.1), they can use a coaxial feed alimentation (figure 2.2) as well. These techniques will be detailed further ahead.

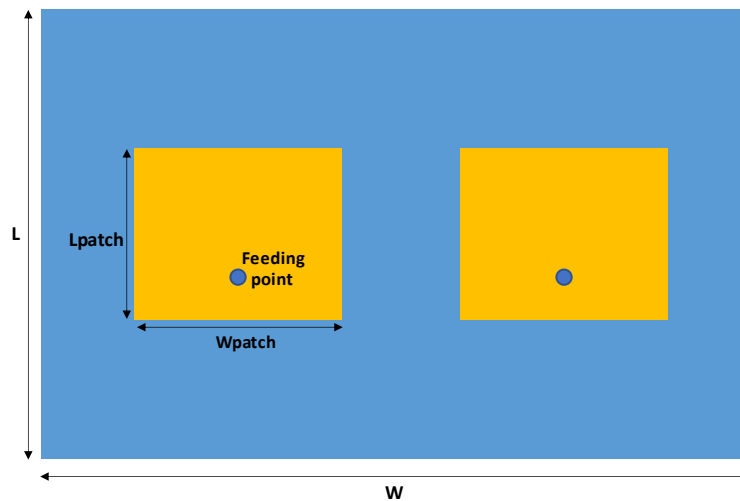


Figure 2.2-Exemple of an antenna array with two elements

2.2 Antenna parameters

After understanding the basic concept of antennas and antenna array, it's also important to have the cognizance of some of their parameters. [3], [4]

- **Gain:** The amount of power transmitted (considering antenna losses) in the main direction of the antenna in respect to an isotropically radiating source.
- **Bandwidth:** Range of frequencies where several parameters such as the input adaptation of the antennas have a good performance when compared with the central frequency characteristics. In this dissertation, the range of frequencies were considered good when the reflection coefficient at the input port of the antennas was -10dB or less.
- **Radiation pattern:** The geometric pattern of the relative strengths of the field emitted by the antenna.
- **ECC (Envelope Correlation Coefficient) :** Isolation and correlation between communication channels (i.e., elements of an antenna array) can be measured by ECC. The ECC tells how independent two radiation diagrams of two antennas are, that is, how much the radiation diagram of one antenna influences the diagram of the other antenna.[5]
- **Realized gain:** It's the gain but considering impedance mismatch loss.
- **DG (Diversity gain):** The amount of the transmission power that can be reduced when using a diversity scheme, which is a method of improving the reliability of a message signal when using two or more communication channels with different characteristics without losing the performance of the system and can also be related to the ECC with the following equation [6].

$$DG = 10\sqrt{1 - (ECC)^2} \quad (2.1)$$
- **Input Impedance:** Ratio of the complex, input voltage and current at the antenna port. Usually, the antenna input impedance should be 50Ω because that's the impedance value of the transmission lines most of the times.

2.3 Design of a single antenna with recessed alimentation

2.3.1 Width and length

The antenna parameters were calculated using the following expressions and equations [9]:

- F_r = central frequency of antenna operation: 8.4GHz
- h = dielectric thickness: 1.6mm
- Conductor thickness: 35 μm of cooper

- ϵ_r = Relative permittivity of the dielectric: 3.66
- $\tan(\delta)$ = Tangent of losses in the dielectric: 0.0037

The width (W) and length (L) of the antenna are:

$$W = \frac{1}{2 \times f_r \times \sqrt{\mu_0 \times \epsilon_0}} \times \sqrt{\frac{2}{\epsilon_r + 1}} = \frac{c}{2 \times f_r} \times \sqrt{\frac{2}{\epsilon_r + 1}} \quad (2.2)$$

$$L = \frac{c}{2 \times f_r \times \sqrt{\epsilon_{eff}}} - 2 \times \Delta L \quad (2.3)$$

Being ΔL the Length extension caused by the fringing effect

$$\Delta L = 0.412 \times \frac{(\epsilon_{eff} + 0.3) \times (\frac{W}{h} + 0.264)}{(\epsilon_{eff} - 0.258) \times (\frac{W}{h} + 0.8)} \quad (2.4)$$

Where the effective dielectric constant is given by:

$$\epsilon_{eff} = \frac{\epsilon_r + 1}{2} + \frac{\epsilon_r - 1}{2} \frac{1}{\sqrt{1 + 12 \frac{h}{W}}} \quad (2.5)$$

2.3.2 Y_0 and power line width of characteristic impedance $Z_0 = 50\Omega$

The input resistance of the antenna patch is given by the following expression for $y = 0$ [9]:

$$R_{in} = 90 \times \frac{\epsilon_r^2}{\epsilon_r - 1} \times \frac{L}{W} \quad (2.6)$$

Since this resistance is different from the circuit resistance input (which is 50Ω), it is necessarily to make the adaptation. This adaptation will be made using to the recessed microstrip-line feed a technique where it will be inserted a microstrip line with a width of W_0 , in a slot of a specifically depth of y_0 . This width will correspond to a 50Ω impedance.

This new expression is given by [9]:

$$R_{in_{50}}(y = y_0) = 50\Omega, R_{in_{50}} = R_{in} \times \cos^2\left(\frac{\pi}{L}y_0\right) \quad (2.7)$$

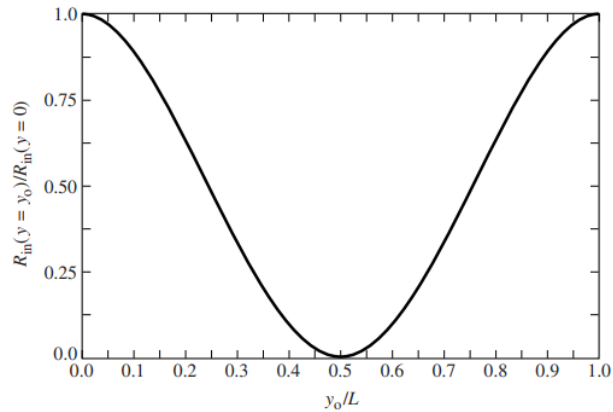


Figure 2.3-Normalized input resistance[7]

Looking at the figure 2.3, it's easily deduced that the minimum value of the normalized input resistance occurs in the middle of the patch length, and it has its maximum in the extremities, so it's possible by an interactive method, to change the position of the feed along the patch, in order to find the physical point where the antenna will be almost perfectly matched with 50Ω . The tool TX LINE was used to find the width W_0 of the 50Ω line being the value used 3mm.

2.3.3 Design of a single antenna with coaxial feed

Another method of feeding the antenna is by using the same strategy of the previous model, however, instead of placing a feed line on the patch, this feed is replaced by a probe feed (figure 2.4) that is inserted on the ground and goes all the way to the top of the patch.

In such manner it's possible to place the antennas wherever wanted over the substrate, so they can be arranged on a certain order without the risk of their feeds touching any other structures, that could be used on the future to reduce the coupling between elements.

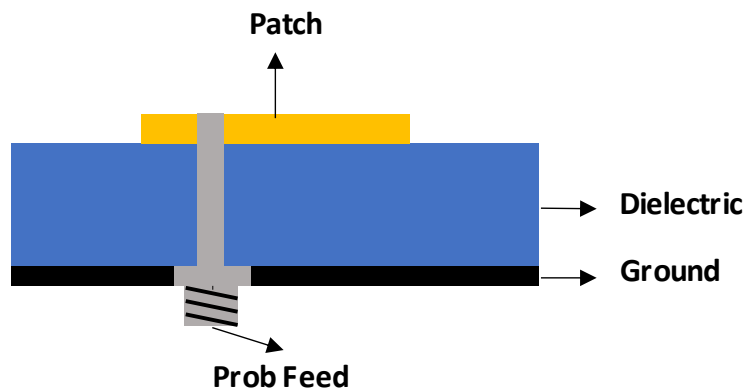


Figure 2.4-Antenna being feed by the coaxial technique

Although the type of feed of the antenna has changed, the expressions to calculate the appropriate dimensions of the rectangular patch are the same as the ones presented on

the 2.3.1 section, and then, using CST Studio Suit utilities, it's possible to get the adequate dimensions of the probe feed to match the impedance of 50Ω .

2.4 Coupling paths for the antenna elements

2.4.1 Transmission mode

In order to have a better comprehension on the mutual coupling between elements, it must be understood the causes that make the energy received by each element of an array change. [8], [9]

There are several factors that impact the energy received by each element, but it can be highlighted some of the most important factors such as:

- The separation between elements
- The orientation of the antennas
- The characteristics of the radiation patterns of the antennas.

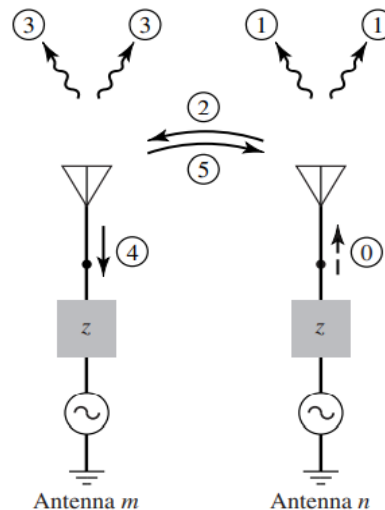


Figure 2.5-Coupling on the transmission mode[7]

By looking at the example above (figure 2.5), let's assume a simple case where the antenna n is excited, and the antenna m is the parasite (assuming the transmission mode).

In that case, the energy that come from the n generator will flow through the whole antenna and will be radiated to the space (1) or will enter through the neighbouring antenna (2). This energy received by the antenna m will go against the generator of its own (4) or will be radiated to the space (3).

In these two cases, the energy is in some way recovered, but it can also be reflected once more to the antenna n .

When both antennas are excited, the radiated and recovered fields are summed together vectorially, this is, the wave that goes from the antenna n to the antenna m generator will be added vectorially to the incident and reflected waves of the antenna m itself.

The vector of the sum of these two waves will influence the input impedance seen from the antenna's m terminals, which will lead to the problems caused by the coupling.

This impedance is known as the driving impedance, which is the impedance seen from a single element when the dissimilar elements are excited.

Basically, the driving point impedance of an element is equal to the sum of the impedance of itself, and the phased mutual impedances between its and the remaining elements, (since its self-impedance is obtained when the other elements are in open circuit, so that the current in the feed of its elements is 0).

It's also important to highlight, that on a linear array with N patch elements equally spaced along the X axis, the field of the antenna array is equal to the field of a single patch multiplied by the array factor.

2.4.2 Receiving mode

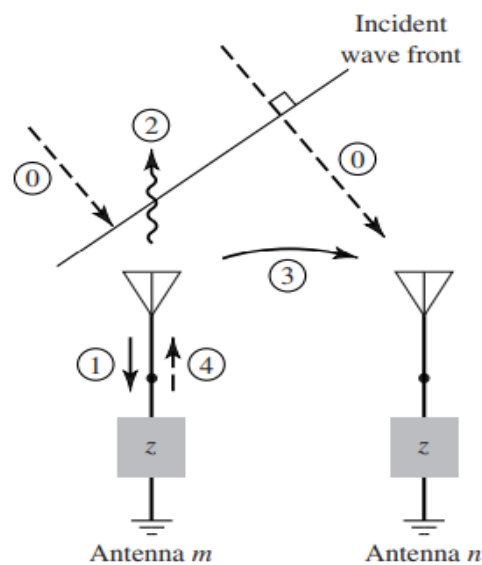


Figure 2.6-Coupling on the receiving mode[7]

On the other hand (in the receiving mode which can be observe on the figure 2.6), when a wave hits antenna m (which will cause current flow), part will be radiated to space (2), and another will go to antenna n (3) which will be vectorially added with the incident wave that hits n (0) and part of it will as well be directed to their feed (1).

Thus, the amount of energy that each antenna receives is related to the vector sum of the direct incident waves and the parasitic waves from the remaining antennas, and this amount of absorbed and radiated energy by each element, also depends on the match made to the impedance terminals.

2.5 Types and other consequences of coupling

After analysing the factors that could greatly vary the energy received by each antenna, it is also possible to acknowledge several factors that could vary the coupling in an array.

Among these factors, these are the most important ones that are included[7]:

- The type of antenna and the design of parameters, since by varying the parameters, it can be varied the impedance of the antennas.
- The reflection coefficients and the patterns of the antennas.
- The type of feed of the antennas.
- The size of the array.
- The type of materials and the thickness of them.
- The space between elements.

Furthermore, the coupling in an array may not come from the same source as it could be different types of coupling. [10]

The antennas have influence over each other through radiation over the air (as it was mentioned previously), or through surface currents that pass through the ground and substrate (because as mentioned on the 2.1 section, in a patch there is a ground that is made of a thin metallic patch of copper printed underneath a substrate).

With that in mind, it can be highlighted three main types of coupling in which each one may be dominant, depending on the type of array and the characteristics of the antennas. These three main types of coupling are surface waves, near fields and spaced waves (figure 2.7).

Surface waves usually dominates when the patches of the array elements are printed on a thick dielectric with a high permittivity, and these waves propagate through the dielectric and undergo diffraction when they reach the dielectric's ground edges.

Near-field coupling happens when one antenna is close to the field of another antenna, so that the field of one antenna is very close to the field of the remaining antenna.

This coupling is dominant in situations where the substrate permittivity is low and in these cases the coupling can cause great degradation in the antenna field.

Finally, there is the space wave coupling, which happens when the antennas are close together, since the total electric field will be normal to the ground, and this will have a high value.

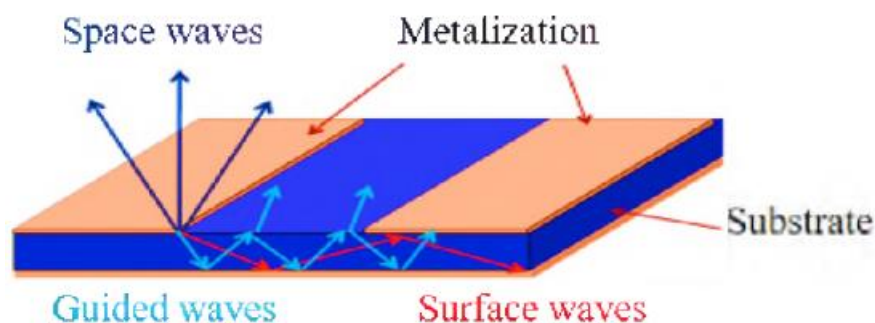


Figure 2.7-Types of waves propagating on the patches that causes coupling[11]

(Note: Increasing a lot the separation between elements on the array reduces the coupling, however it increases the secondary lobes which it can also not be ideal. [12])

2.6 Scan blindness

Another consequence of mutual coupling is the variation in the input reflection coefficient and the input impedance with the scan angle.[7]

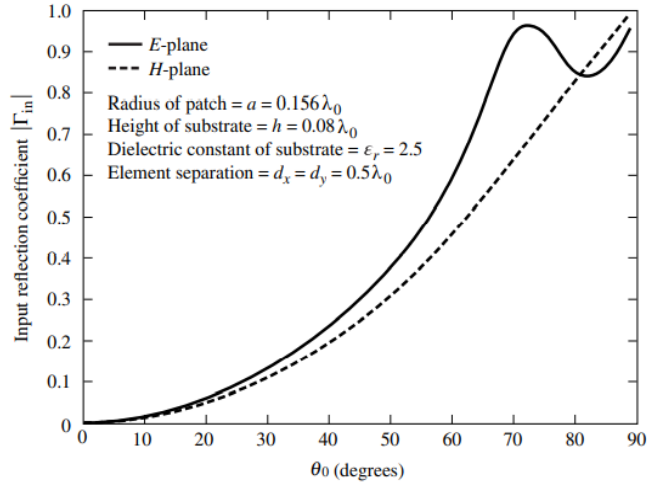


Figure 2.8-Variation of the input reflection coefficient with the angle[7]

The variations in the figure 2.8, are due to coupling and are most noticeable in the electrical field.

Large changes in the reflection coefficient can lead to the so-called array scan blindness which is what is happening there at 73°, these imbalances happen because the waves (in this case called leaky wave) that are not excited enough in relation to the scan angle, these waves being a kind of slow waves.

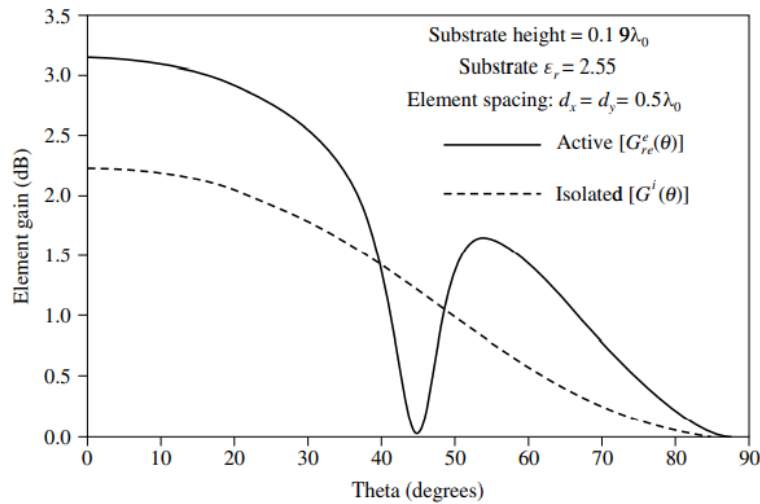


Figure 2.9-Variance of the gain with the angle[7]

Moreover, in a second experiment [7], the authors varied the gain according to the scan angle and once again found that there was a null at 45° (figure 2.9) due to the scan

blindness being the reflection coefficient almost unity, this scan blindness being due to the surface waves.

Additionally, it was concluded by the authors that, however, the gain of the elements when they are isolated do not present any null and the patterns of the isolated elements are also different from when they operate in an array, which proves that the coupling can greatly affect the performance of the array.

Having a specific angle on the antenna array where the gain is null can strongly influence its application for beamforming systems as they rely on putting the antennas radiating at a specific angle.

On another study [13] it was concluded that the radiation diagram performances on traditional dielectric substrates, are hampered by surface waves (which occur due to array excitation or variation in excitation between elements), supported by the substrate itself, which affect the radiation efficiency and increase coupling.

In these conventional dielectrics, it could also be present the scan blindness, which limits the array's scan range, since there will be a misalignment at the input, at a certain angle.

At this angle, the mode of the periodic structure (which is being excited by the array) becomes complex as the array is made to radiate.

When this occurs, the field is propagating and attenuating throughout all the array at the same time, resulting in energy loss through the substrate and in a big mismatch to the array-entry.

2.7 Effects of coupling using the RWG method

In a mathematical analysis [14] using the method of moments and the RWG (Rao-Wilton-Glisson) method (which consists of dividing the antenna surface into small triangles so that the current distribution and antenna patterns can be analysed in any type of antenna) it is concluded, comparing with the ideal scenario, that with coupling there is a lot of reduction in antenna gain and that there may also be a change in the antenna patterns.

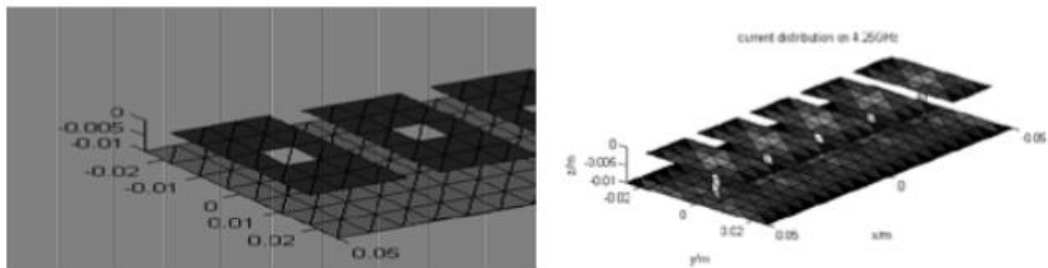


Figure 2.10-RWG method on an antenna array

These examples (figure 2.10) were considered for when the patch elements were very close together, however, when they were at great distances the coupling was negligible furthermore it was also concluded that the mutual coupling can be seen as a mutual impedance.

2.6 State of art-Previous techniques to reduce the coupling.

2.6.1 Electromagnetic band-gap (EBG)

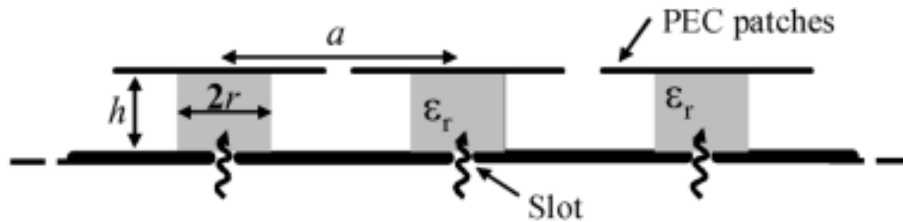


Figure 2.11-EBG structure

On EBG structures (figure 2.11), which is used as the substrate and as the radiating array, they gap the design frequency, so no guided wave will be supported by the structure at that frequency, and the power will not be lost in the form of surface waves [15]. In this new structure both the substrate and the patches are used to make the gap. If patches and substrates are drawn at the same time, with the distance between antennas matching the lattice pitch, the gap performance is good such that surface waves are blocked even if the antennas are close together. In this way, the antennas can be closer together, preventing the occurrence of lobes.

After that, it was concluded that the surface waves may be suppressed with the correct sizing of the array, furthermore with this array the scan blindness does not occur for all phase angles along the E and H planes.

Other articles (such as [16]) mention that despite reducing the coupling between antennas, this structure has the great disadvantage of being complex structure to be developed and applied to arrays in real situations, and it can cause losses in the electrical domain, in addition to which it may not be the best structure to make use of space so that the array is as compact as possible.

2.6.2 Defected Ground Structure (DGS)

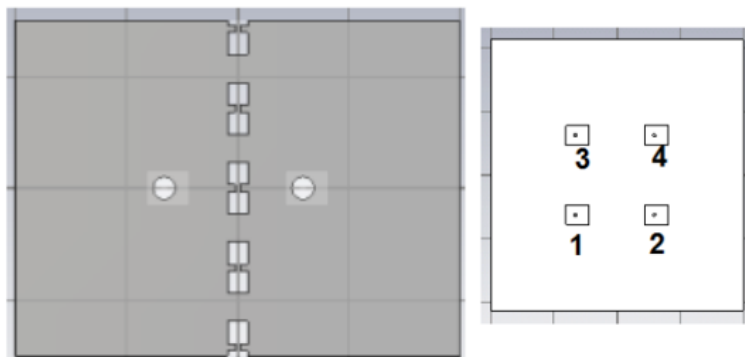


Figure 2.12-DGS structure

The DGS (figure 2.12) has the advantage over EBG of producing the same bandwidth of rejection, however it is a much more compact structure in terms of size and is easier to

implement [15]. This DGS is inserted between the adjacent field of the electric field (by way of explanation, it is basically an opening that is made in the ground of the array in the shape of a gym dumbbell to reduce surface waves and cross polarization between the antennas).

The way this dumbbell works is: the currents that circulate in the ground and that are induced by the surface waves causes the coupling.

With the presence of these structures, it will be disturbed the circulation of these currents in the ground, since a part of the currents that will pass and leave through the DGS, leaves in the form of a displacement current (which forms a capacitor around the gap i.e. it is the intermediate point g and w of the figure 2.13), and another portion will be reflected back as it will go around the arms of the DGS (i.e. it passes through b goes to the a , then goes to the opposite side of b and returns to the starting point), thus forming an inductance that will increase with the increase of the path traveled by the current.

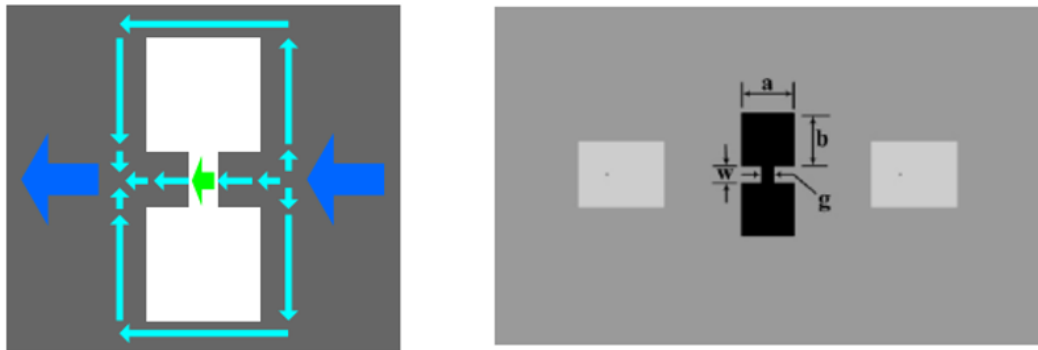


Figure 2.13-current flowing through DGS, and DGS schematic

After tests were carried out on several arrays, there was a decrease in the coupling, that is, in the S_{21} , by about 20dB on average, however, it was also verified that there were some changes in the radiation diagrams and the gain and efficiency of the array decreases as well, which is not ideal. Furthermore, these structures require a lot of trial and error to find the correct dimensions, since as it is a recent technology, fixed expressions for their dimensions have not yet been found.

2.6.3 Meander line

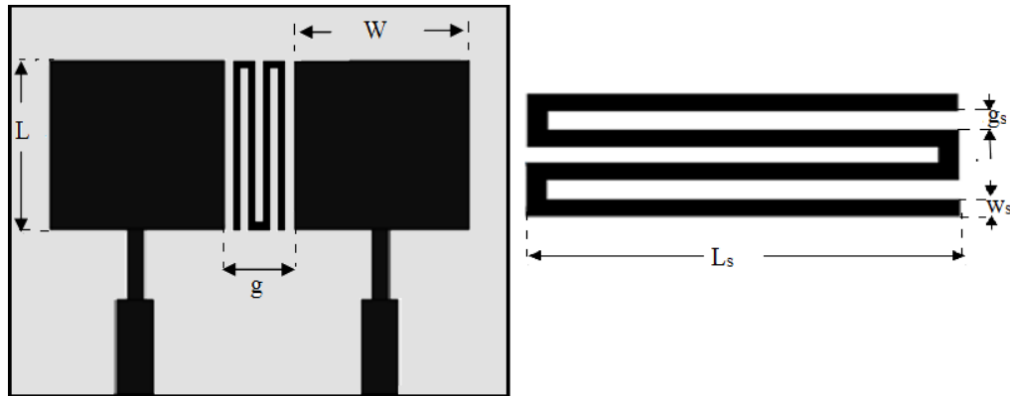


Figure 2.14-Meander line schematic

On an introduction, the authors stated that certain structures are easier to implement but can compromise array gain as well as radiation diagrams. [17]

The best structures that do the most coupling reduction without compromising the array are very complex to implement. So, they introduce a new concept that's the meander line which is a resonant component to make an isolation between the elements with a minimum level of polar power to be crossed. It was found that with an edge-to-edge distance, g of $\lambda/18$ it was possible to obtain a good isolation and that the value of g_s and w_s would be 0.5mm.

The focus of this meander line (figure 2.14) is directed to the coupling of the air, that is, the coupling caused by the proximity of the two fields. By using this structure, is being added an indirect path through which the coupling will pass, that is, instead of the signal being radiated from the antenna 1 to antenna 2, it will be radiated to this intermediate line.

The authors refer that one of the negative causes of mutual coupling is the degradation of the radiation diagrams, therefore, by adding four arms to the intermediate structure, it is possible to have two currents circulating in the opposite direction, so that when the radiation diagrams of this structure add to the final radiation diagram, the radiation diagram of this structure is cancelled thus preventing the array radiation diagram from changing.

It is concluded that with this structure it was possible to reduce the coupling between elements that is the S_{21} , in 10dB, that is close to a value provided by some EBG structures, but with a much lower complexity. Besides the advantages presented previously, once more, these structures need some trial error to get a precise result.

2.6.4 Metamaterial

It's mentioned that these materials can offer a negative permittivity and/or permeability, which can be used to manipulate the circulation of the surface currents on the substrate. [18]

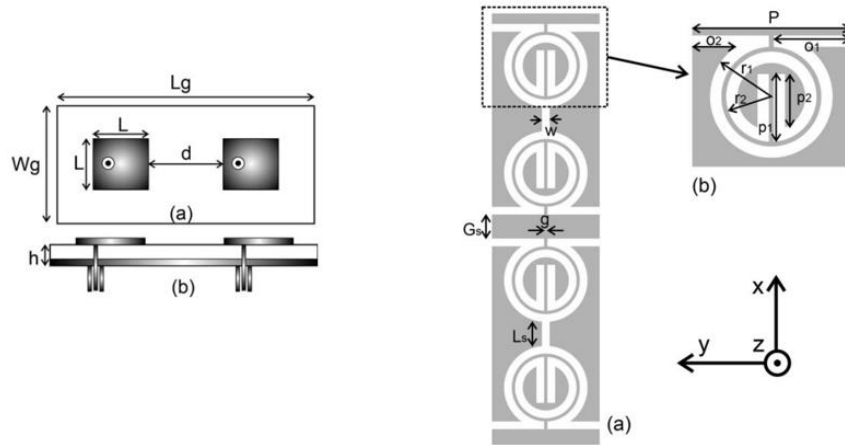


Figure 2.15-CSRR schematic

In the example of the figure 2.15, two antennas were placed at 0.125λ apart, with the purpose of them being very close together to obtain a strong coupling, being the coupling that took place was due to the surface waves.

The CSRR (Complementary Split Ring Resonator) is a ring which is manufactured in such a way to cancel out the electric fields and the surface waves, however once again the antenna gain decreases.

In the state of the art of another studies [19][20] the authors mention that there are several techniques that have already been used and that managed to reduce the coupling such as EBG, FSS (Frequency Selective Surface), SNG (Single Negative Gaps), however these components are relatively large.

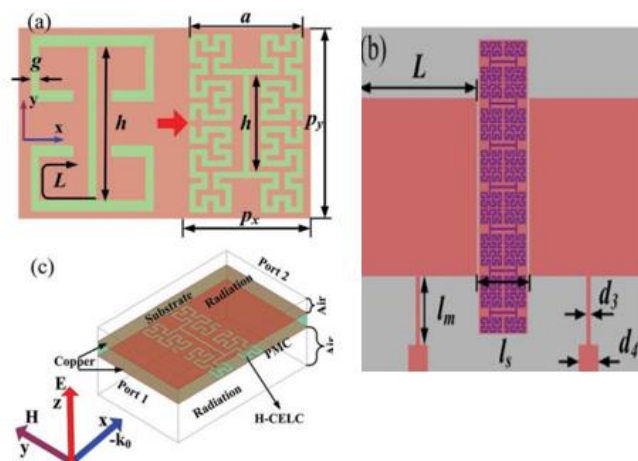


Figure 2.16-Metamaterial with a Hilbert design[20]

The authors present the mathematical waveguide (figure 2.16) for the reduction of the electromagnetic coupling that operates on a $\lambda/8$ spacing.

WG-WTM are artificial materials made of two parallel metal plates that are embedded in periodic cells. These cells with a substrate in between forming the medium for the guided waves to pass through.

With that in mind, they put these structures in the middle of the elements to suppress the surface waves.

The space waves that are responsible for the electromagnetic coupling in both the E field and the H field are once again captured by the structure and converted into surface currents that are also attenuated by the structure.

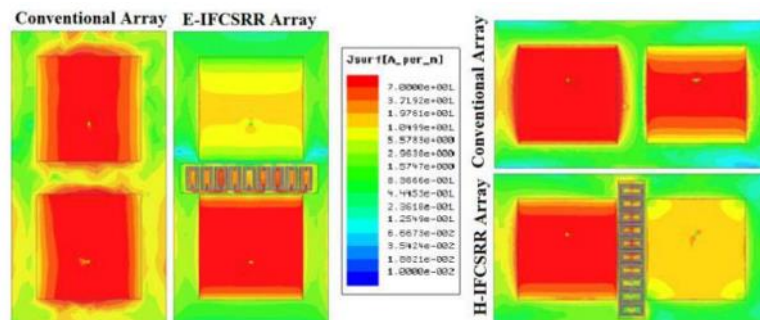


Figure 2.17-Effects of current on the structures[19]

In the figure 2.17, it is possible to see that the surface currents reduces both in the E field and on the H field when it's compared the currents with and without the WG-MTM (Waveguide Metamaterial) which led to a coupling decrease.

3. Metamaterials

This chapter analyses metamaterial structures, it's discussed how and why they can reduce mutual coupling between antenna elements.

Initially it's putted in perspective why these structures have so an important rule to reduce the MC by understanding the impact of it's unusual features.

After that, it's shown how they can be design in order to achieve the desired properties at a desired frequency.

3.1 Motivation to use metamaterials

After analysing some of the structures that exists today (which were presented on the **section 2.6**), it was concluded that in order to reduce the MC it would have to exist to some extent, a trade off in some aspects on the parameters of the antenna patches, that is, it would have to be made a structure that didn't compromise the gain, the efficiency, the radiation diagrams of the patch, and at the same time, it should not be a very complex structure and could be compacted on an antenna array.

For that reason, it was chosen to be analysed the metamaterials, due to their promising features that are on the rise in the current market.

3.2 Fundamental concepts of metamaterials

3.2.1 Properties of metamaterials

As mentioned before, one of the big causes of coupling is due to surface currents on the substrate, so the coupling between two elements can be reduced by supressing the surface waves.

They may be cancelled out by properly adding an extra indirect coupling path so it should be created an indirect signal coming via the extra coupling path that opposes the signal going directly from element to element. If the two amplitudes are comparable, the two signals add up destructively, and the mutual coupling is reduced.[21]

In addition to that, the extra coupling path needs, as well, to change the directions of the currents on the antenna array so the current generated by one element doesn't reach the remaining elements.

In order to create a signal that opposes the phase signal of the current flowing from one antenna element to another and also changes the current direction, it must be looked first to the fundamentals of the light's signal's transmission regarding a reflexion/refraction situation[22].

In normal situations (figure 3.1), when a signal hit's an external medium/objected, part of the incoming signal will be reflected and the other part will be refracted (i.e., transmitted), and although this new transmitted signal has a different angle, it maintains the same direction.

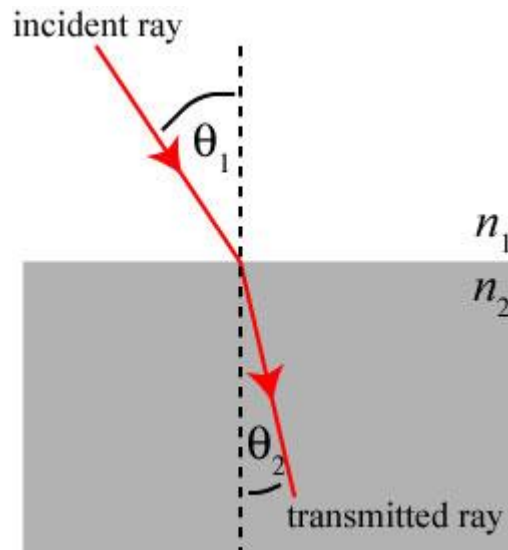


Figure 3.1-Schematic of a normal refraction[23]

However, this only happens when the refraction index of the second medium is positive. So, in order to create a medium where the refracted signal opposes the incoming signal, the second medium must have a negative refraction index (figure 3.2).

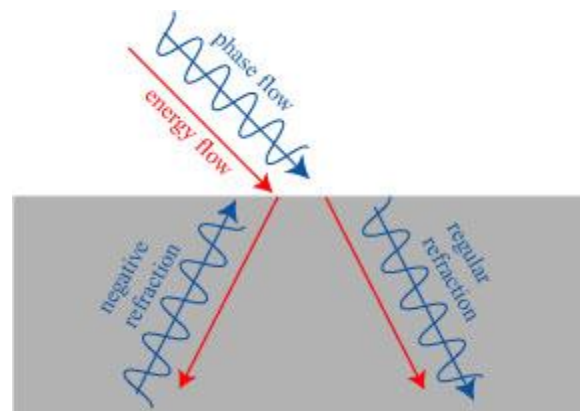


Figure 3.2-Schematic of a negative refraction[23]

Looking once again to the basics of the transmission signal's rules, the only way to achieve a medium where the refraction index is negative, is by having a medium where the magnetic permeability and/or the electric permittivity are/is negative whereas the Snell's law defines it:

$$n = \frac{\sin \phi_1}{\sin \phi_2} = \frac{n_2}{n_1} = \sqrt{\frac{\mu_2 \epsilon_2}{\mu_1 \epsilon_1}} \quad (3.1)$$

- n : Refractive Index of an optical medium.
- ϕ_1 : Angle of incidence.
- ϕ_2 : Angle of refraction.
- n_1 : Refractive index of the first medium.
- n_2 : Refractive index of the second medium.
- μ_1 : permeability of the first medium.
- μ_2 : permeability of the second medium.
- ϵ_1 : permittivity of the first medium.
- ϵ_2 : permittivity of the second medium.

Most of the materials encountered on the nature have both positive permeability and positive permittivity. However, if certain materials are disposed in a certain order, it can be achieved the desired negative values of both the permeability and permittivity and oppose the incoming and refracted signal (i.e., opposing the currents on the antenna array). This new material is called a metamaterial.

After understanding how this extra path created by metamaterials will make a medium that allows the currents generated by of one the antenna's array to not reach the neighbouring antennas, it's also crucial to acknowledge why the amplitudes of the indirect signal coming via the extra coupling path, that opposes the signal going directly from antenna to antenna will add up destructively.

Looking over the Poyting vector law, if the permittivity and the permeability of the medium are positive, the direction of Poyting vector, that in this case is the direction of the current flow, is the same as the direction of the propagation vector, that in this case is the direction of phase advancement, which is the characterization of a Right-Handed Medium (figure 3.3) [22].

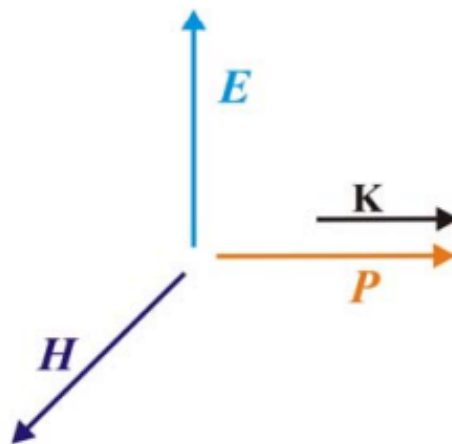


Figure 3.3-Illustrations of directions of electric field, magnetic field, Poyting vector and wave vector on a Right-Handed Medium[24]

Nonetheless, when the permittivity and the permeability of the medium are negative, the direction of power flow and the direction of phase advancement are opposite from each other, which is the characterization of a Left-Handed Medium (figure 3.4) [22]

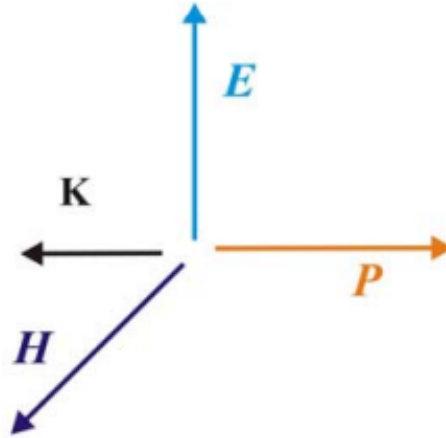


Figure 3.4-Illustrations of directions of electric field, magnetic field, Poynting vector and wave vector on a Left-Handed Medium[24]

With this concept of the Poynting vector in mind, it's possible to conclude that the amplitudes of the indirect signal coming via the extra coupling path, that opposes the signal going directly from antenna to antenna will add up destructively.

In addition to what was explained before, it lay emphasis on the fact that these artificial materials, with negative refractive index, have frequency-dependent values of ϵ and μ , that is, they are dispersive media, being simultaneously negative within a specific frequency band.[25]

Now that is clear why it's important to generate a secondary medium with a negative index, it must be understood the way this negative index is created by these metamaterials, which will be explained further ahead of this work, however, it is necessary to first, look at design of it.

3.2.2 Design of metamaterials

This extra element called metamaterials, that could change the currents of the structures must fit the antenna array, and they started being analysed a lot of decades ago.

Initially the main design requirement was to secure a space in the design, in which an electric field could interact with a drifting longitudinal electron object, so the resonance was obtained based on the parts of a metallic structure, which can be identified as an inductance and a capacitance.[26]

The capacitance is given by opposing metallic grids (i.e., by a gap) and the inductance is provided by the rest of the cavity (this inductance being the result of the horizontal current flowing in the structure).

Thus, there was an interaction space where the field affects the movement of electrons and vice versa, when the electrons have supplied energy to the field (figure 3.5).

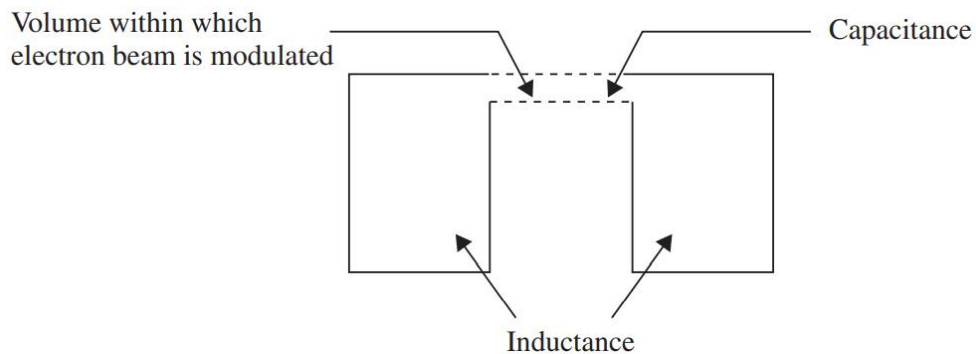


Figure 3.5-Re-entrant cavity[26]

On top of that, metamaterials should be accessible to the electric and/or magnetic fields, and are comparable to most modern resonant circuits used nowadays, this is:

- They are an open structure that are small in relation to the wavelength.
- Furthermore, they have a slot through which the resonant circuit can interact with external fields.
- Their frequency of resonances is determined by the capacitance and inductance of the resonant circuit.

In general, to have an artificial magnetic behaviour, it is necessary to have a geometric shape in which the induced currents are distributed, in a very uniform manner, which can be obtained by **spirals or loops**, thus producing a strong magnetic moment.

On this loop, if the electric field is applied perpendicular to the gap, the positive charges will be pushed in the direction of the electric field, so the opposite sides of the gaps become charged contrariwise, this is, one is negative, and the other one is positive, consequently the gap becomes a capacitor.

Because the current flows all the way through the loop, it's also created an inductive effect, so the loop becomes an LC (Tuned Circuit) resonator with negative permittivity.

Moreover, if the magnetic field is applied perpendicular to the plane of those loops, currents will flow in this loop due to the magnetic induction effect creating a negative permeability.[22]

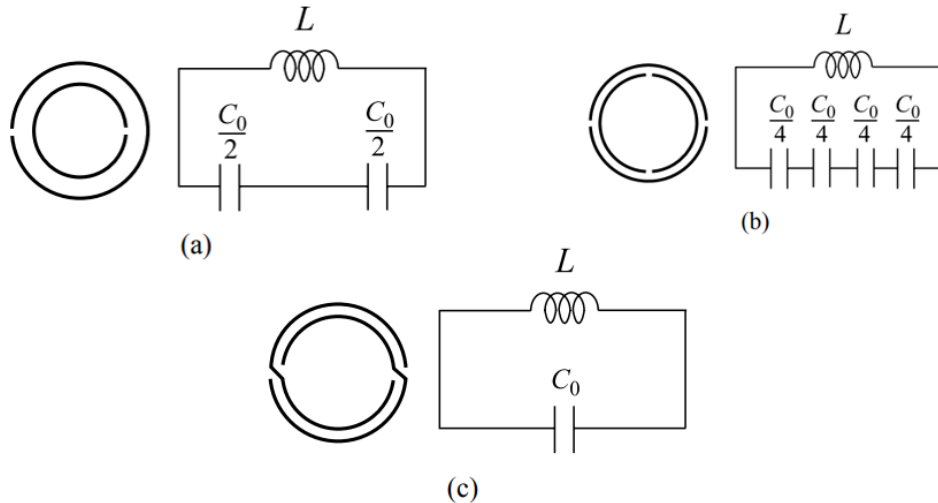


Figure 3.6-Equivalent circuits of different metamaterials[26]

The loops of the metamaterials could have more than one gap, which will result in more capacitors in the loop, which will lead to a different resonant frequency.

In example B) of the figure 3.6, the ring has four sections, so there are four capacitances in series, each of these four capacitances having an equivalent value of $C_0/4$ and being C_0 the total capacitance of the ring.

With the same size, example C) has the lowest resonant frequency because the resulting capacitance is the highest. The authors performed tests and concluded that for the same size, the SRR (Single Ring Resonator) B) had approximately twice the resonant frequency of the SRR on example A).

On top of that, after a lot of experimental tests, it was concluded that by joining the gaps, there's an increase in capacitance, that is, the resonant frequency decreases and by adding one more gap the total capacitance is being separated, so the resulting capacitance will be smaller, which leads to a higher resonant frequency.

What is more, by having gaps, will allow the metamaterial to be excited by the electric and/or the magnetic field (depending on how these fields are parallel or perpendicular to the gaps), so it's fundamental that these structures **have at least one gap**.

After analysing the gaps, it's also important to define the loops of the metamaterials. These loops can be made using cooper, and the plane under them, the substrate (this combination is called SRR), or the opposite, where the loop is created by the substrate and the rest is covered by cooper (this combination is called CSRR).

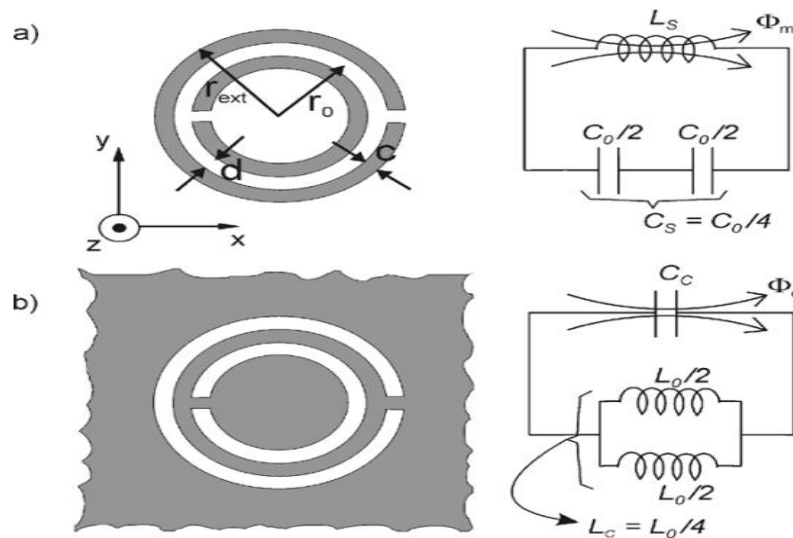


Figure 3.7-Equivalent circuits of SRR and CSRR[27]

In the circuits of the figure 3.7, it's possible to ascertain, that the metal and air have been exchanged, hence the name complementary SRR (CSRR), however it has been deduced that the resonant frequency appears at approximately the same frequency, as its expected from duality.

That's because in CSRR, there's a behaviour of an electric dipole excited by an axial electric field, whereas in the SRR it has a resonant magnetic dipole excited by an axial magnetic field.

Besides the fact that these structures are different, they can be analysed in the same way since they are the dual of each other, that is, in CSRR its feasible to change the space between the gaps, and be under the impression that it's being changed the capacitance as in the SRR (even if it's being changed the inductance it can be seen otherwise, since these are the dual of each other and theoretically they will behave similarly).[27]

After analysing the loops and the gaps of the metamaterial, it's time to talk about the geometry of them. Metamaterials have not a restricted guide regarding the design, as long as it obeys to rules talked previously: they have to be loops to provide the inductance, and surfaces close together to provide the capacitance.

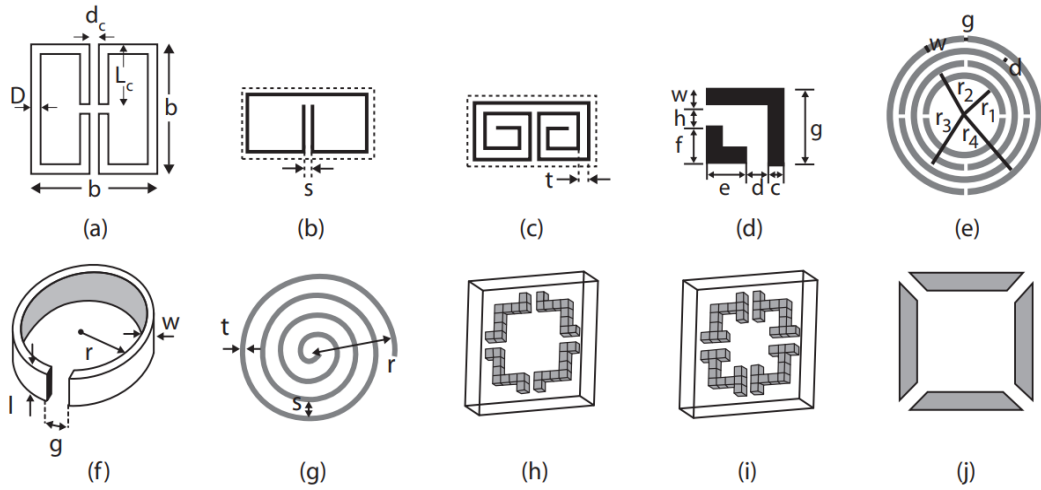


Figure 3.8-Examples of different metamaterials [27]

In the figure 3.8, it's possible to observe a lot of several designs of metamaterials however they all obey the basic rules mentioned previously.

4. Simulated Results

In the fourth chapter it will be presented the design and mode of simulation of the two metamaterials proposed individually, as well as the results and comparisons of the implementation of them in the antenna arrays.

In this chapter all the results were obtained in simulator CST and the antennas array had 2 elements each.

4.1 Design and simulation of the metamaterials

Firstly, is important to note that the designs did not follow a specific formula to be made. Although there are some formulas and expressions in the literature to made specific metamaterials, these are approximations, so there is not a fixed formula to design it 100% accurate.

Aiming to design these metamaterials, it was used an iterative process where it was played with the dimensions of each metamaterial and the sizes of the gaps, but at each moment it was kept in mind that these dimensions needed to be small in relation to the wavelength, had gaps, needed to be geometrically loops, and got to be made of cooper and substrate which gave a good and clear starting point

The first metamaterial that was created is a variation of a CSRR U shape metamaterial (figure 4.1)[5]. These types of metamaterials have the advantage of not being very complex to design and due to its geometry, the signals cancel out (which was the point of what was explained through all the section 3.2), so the radiation diagram does not degenerate.

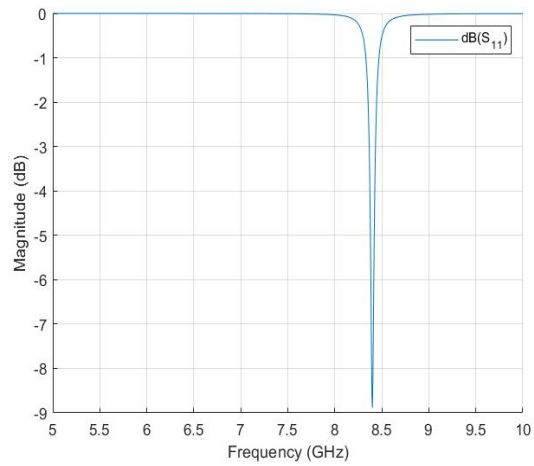
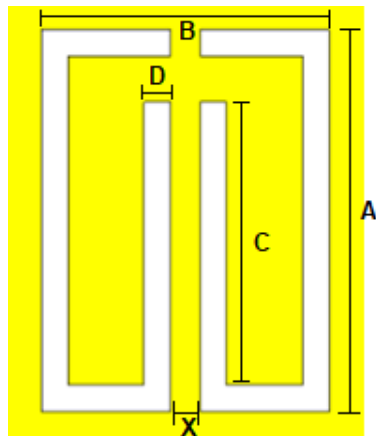


Figure 4.1-2D plan and equivalent resonant frequency of the variation of a square metamaterial

A	B	C	D	X
5.3mm	4mm	4.3mm	0.367mm	0.41mm

Table 4.1-Values of the square metamaterial parameters

Observing the figure 4.2 it's possible to acknowledge that by changing the dimensions of the capacitor gap, which is the X variable, the minimum value of the metamaterial goes up in frequency.

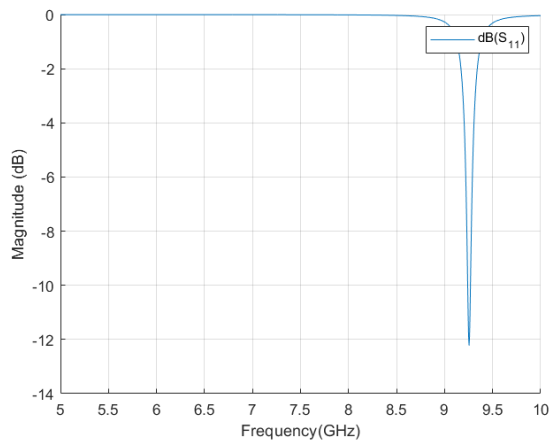
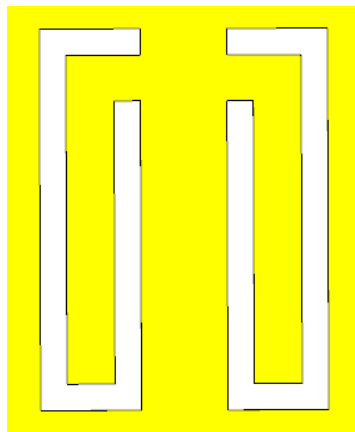


Figure 4.2-2D plan and equivalent resonant frequency of the variation of a U shape metamaterial with an X of 1.2mm

On the other hand, if the variable C that is the one who controls the gap capacitance, the minimum value of the metamaterial goes down in frequency (figure 4.3).

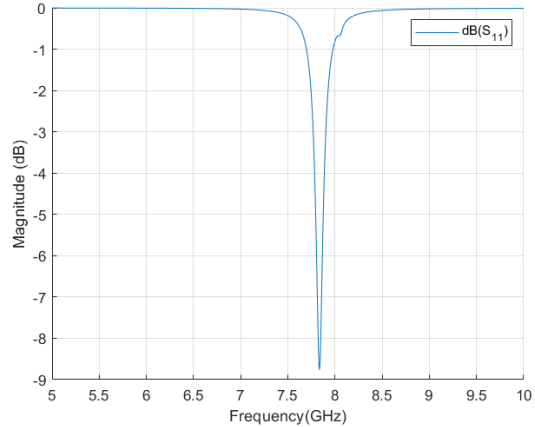
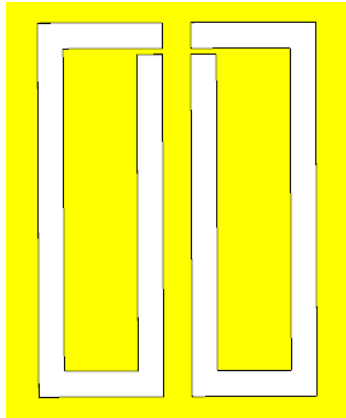


Figure 4.3-2D plan an equivalent resonant frequency of the variation of a U shape metamaterial with an C of 4.5mm

In order to see the minimum value of the metamaterials when these were isolated, it was defined the conditions off the unit cell (basic block of the periodic structure) to Floquet port mode (figure 4.4) which is the ideal mode to analyse periodic structures.[28]

The construction of unit cells for metamaterial simulations can be done using linked boundaries and two Floquet ports, with one port above the plane of the structure and the other port under it, or only with one port above the plane, being the applied excitations the Floquet modes themselves.

As a result of the field solution, the reflection properties of the metamaterial are molded in terms of the computed S-matrix entries.[28]

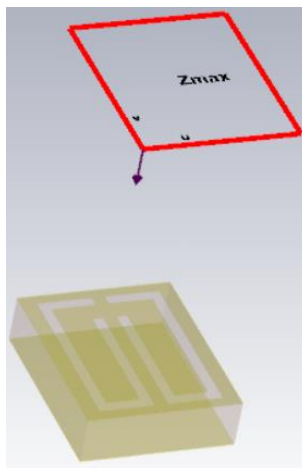


Figure 4.4-Floquet port mode of the unit cell

As mentioned previously, this metamaterial prevents the radiation pattern to not degenerate. That happens due to the fact of the currents flowing in the arms of the capacitor gap have an opposite course (figure 4.5) which makes the Fairfield of the periodic structure to be cancelled by each other avoiding negative effects.[21]

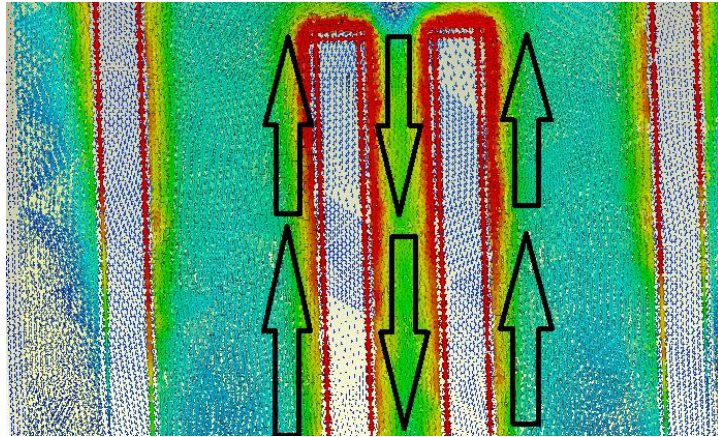


Figure 4.5-Flow of the currents on the U-Shape metamaterial arms

The second metamaterial that was created, is a variation of a double ring shape metamaterial (figure 4.6). This type of metamaterial is a variant of the traditional metamaterial rings that are explored on the literature. [26]

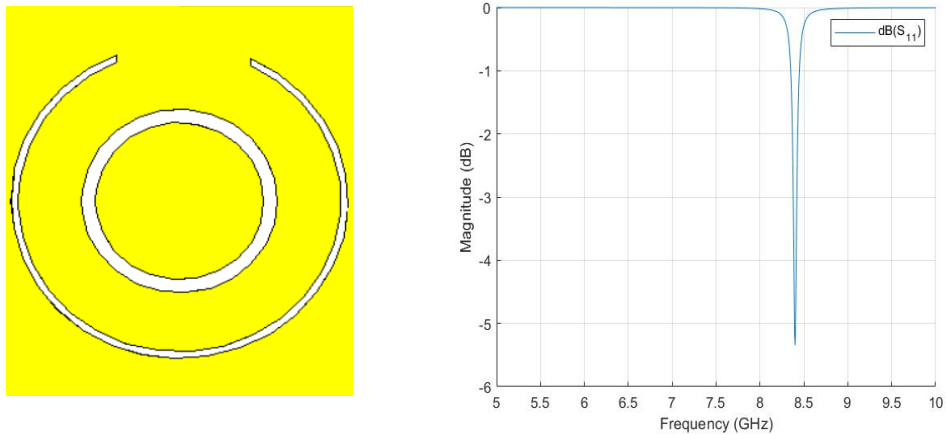


Figure 4.6-2D plan and equivalent resonant frequency of the variation of a two ring metamaterial

Major Rout	Minor Rout	Major Rin	Minor Rin	Gap
2.4mm	2.3mm	1.4mm	1.2mm	~1.9mm

Table 4.2-Values of the circular metamaterial parameters

By looking at the figure 4.7, it can be concluded that when the outer ring is brought closer to the inner ring, making the two rings closer to each other, the minimum value of the metamaterial is greater than 8.4GHz.

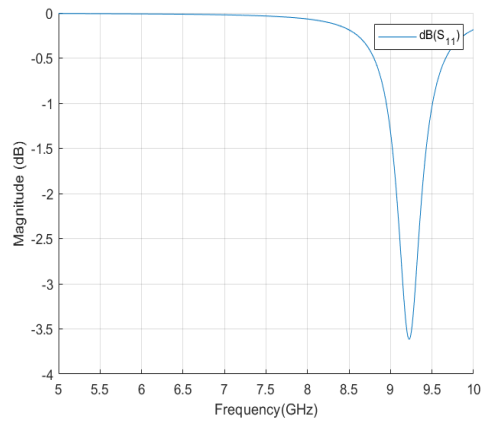
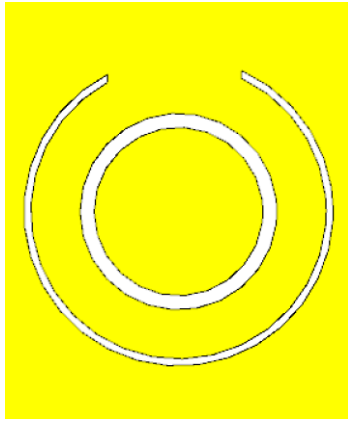


Figure 4.7-2D plan and equivalent resonant frequency of the variation of a two ring metamaterial with the rings closer

At the same time, if the distance between rings is maintained, but the size is enlarged, the resonant frequency also raises (figure 4.8).[28]

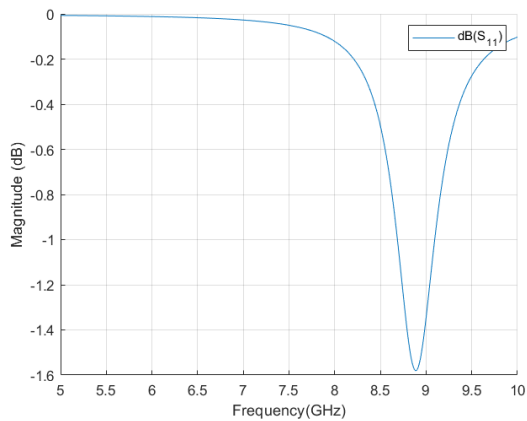
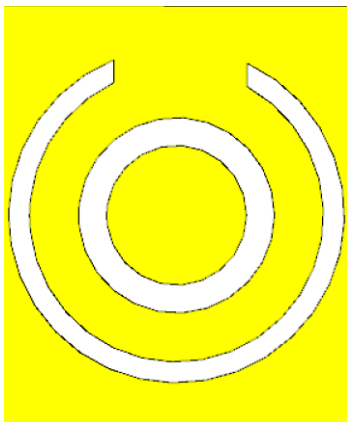


Figure 4.8-2D plan and equivalent resonant frequency of the variation of a two ring metamaterial with the size of the rings enlarged

The same concept in regard to the degradation of the radiation pattern applied on the previous structure is valid once again to this metamaterial as it can be observed on the figure 4.9.

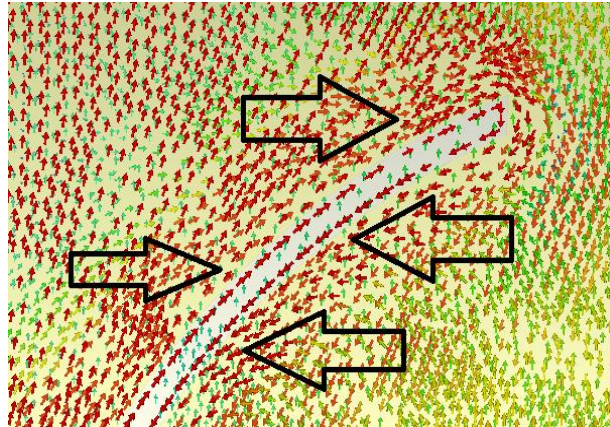


Figure 4.9-Flow of the currents on the double ring metamaterial arms

4.2 Simulated results

4.2.1 U Shape metamaterial in an array with coaxial feed

As it's possible to see on the figure 4.10, when the elements were spaced by 0.5λ and with the metamaterial, the coupling was reduced at around 8.4 GHz on the two element antenna array, being the maximum reduction approximately 23 dB, which was desirable and expected. It's important to mention that both the S21 and S12 are equal so in the figure it's only presented the comparisons between the S21.

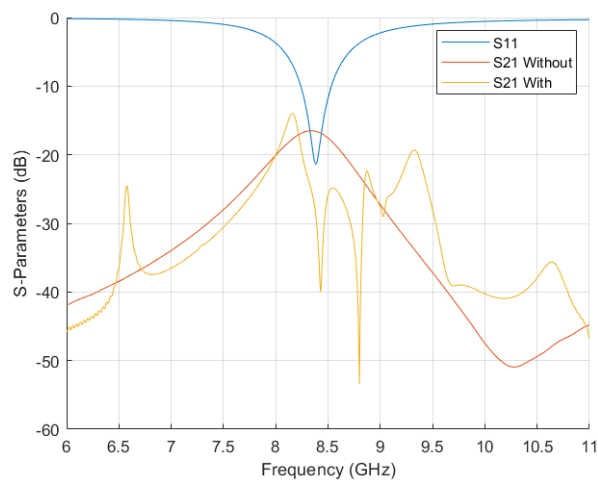


Figure 4.10-S21 with and without metamaterial

In regard to the Total efficiency (figure 4.11), it can be seen that there are practically no changes with and without the metamaterial however with metamaterial it is a little bit better (at around 8.4 GHz as the frequency shifts a little bit with the insertion of the metamaterials).

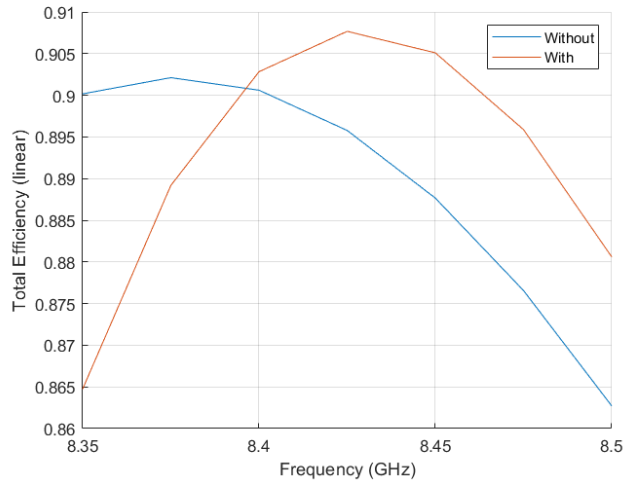


Figure 4.11-Total Efficiency with and without metamaterial

Also, as it's possible to observe, when the metamaterial is added to the array, the diagrams of radiation (figure 4.12) didn't suffer major changes which is desirable.

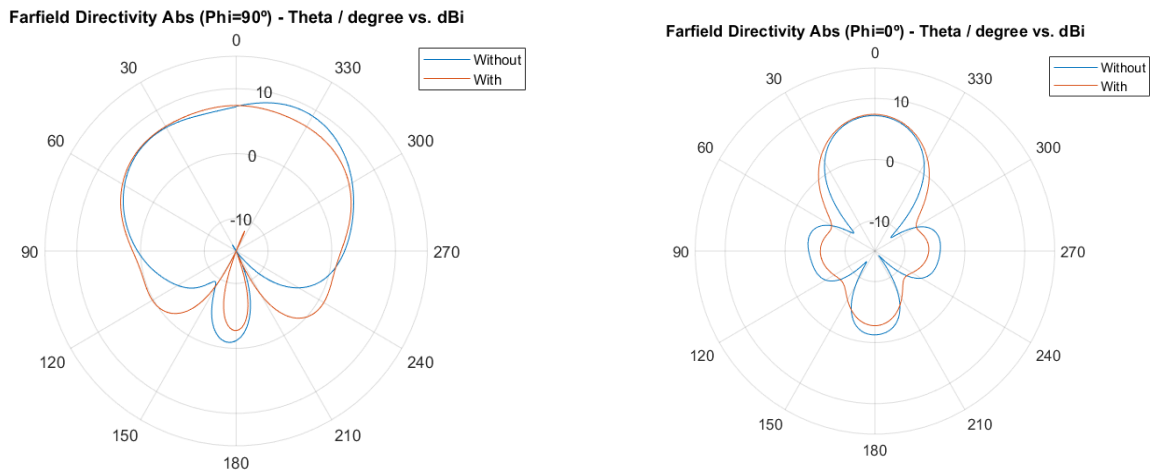


Figure 4.12 -Diagrams of radiation with and without the metamaterial

The ECC and diversity Gain (figure 4.13) had a little bit of improvements however when comparing the two there is not a big of a difference, which reinforces the fact that the metamaterial doesn't compromise the performance of the MIMO array in regard to its diagrams, in view of the fact that the lower the ECC is, the best performance of the diagrams there is.

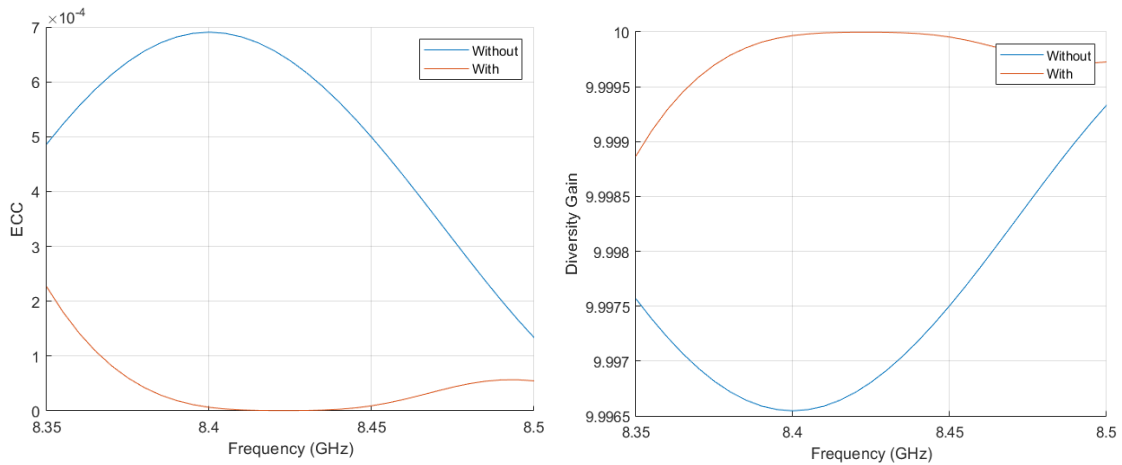


Figure 4.13-ECC and Diversity Gain with and without metamaterial

In spite of the fact that the improvements of the ECC and diversity Gain were not very high in these cases, it can have a higher impact in bigger antenna arrays or in antenna arrays where the feed method of the antennas is different.

In regard to the scan blindness, it had minimum changes with the periodic structure on the array, still, without the metamaterial it was already inconspicuous so it will not be presented here, nonetheless, in bigger MIMO systems/MIMO systems where the coupling is more pronounced, it could have a bigger impact, so it's always a factor to keep in mind as it can compromise a beamforming usability.

One more important point to reinforce, is that what lead to the decrease in coupling was the decrease of the surface currents (and not the other way around).

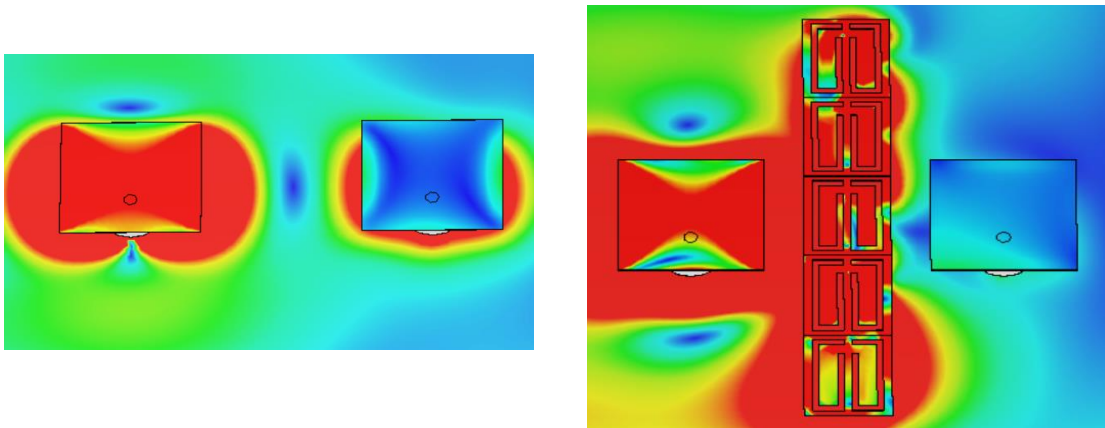


Figure 4.14-Surface currents (0 to 3A/m) without and with the metamaterial

This decrease in the surface currents (figure 4.14) was possible due to the fact that the metamaterial changed the path of the currents (which was the main goal of these structures as mentioned on the **3.2.1 section**).

Observing the following images, it's possible to acknowledge that when the periodic structure was on the array (figure 4.16), the direction of the adjacent currents (this is the currents on the left side of the left antenna and the currents of the right side of the right

antenna) were the same. On the other hand, when the metamaterial was not on the array (figure 4.15), these currents have opposite directions which lead to an undesirable effect of the currents.

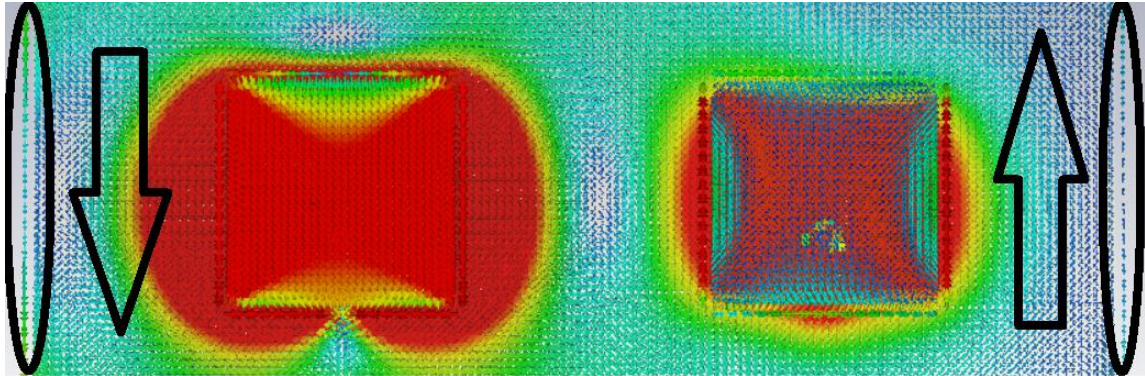


Figure 4.15-Direction of the adjacent currents without the metamaterial

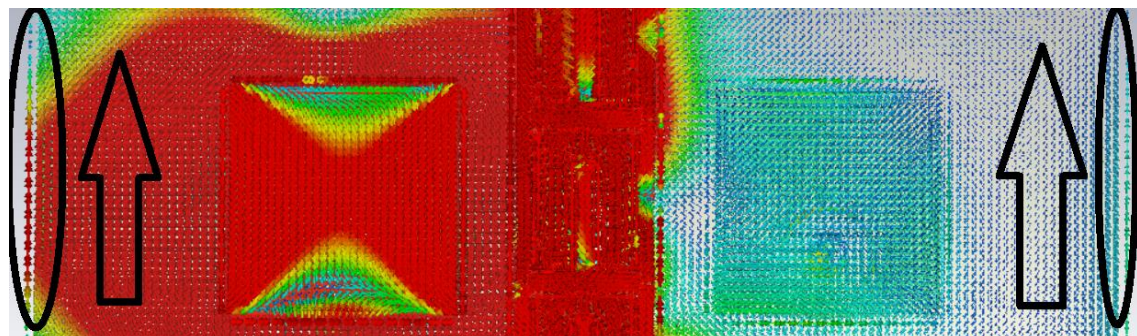


Figure 4.16-Direction of the adjacent currents with the metamaterial

4.2.2 Double ring metamaterial in an array with coaxial feed

Comparing once more the coupling of the two element antenna array with and without the metamaterials, it can be seen that with the metamaterial the coupling was again reduced at around 8.4 GHz, however, this time the maximum reduction was not approximately 23 dB, but around 10dB (figure 4.17) which makes this metamaterial also good, but not as great as the previous one.

This reduction is again due to the reduction of the effect of the surface currents.

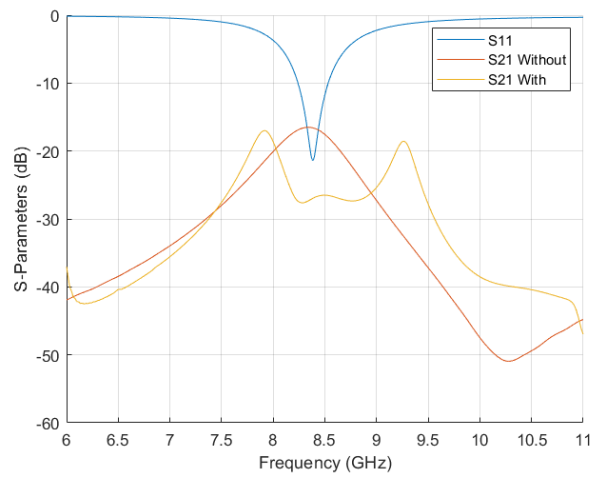


Figure 4.17-S21 with and without metamaterial

Afresh, analysing the total efficiency (figure 4.18) of the array it's concluded that with and without the metamaterial, it is about the same.

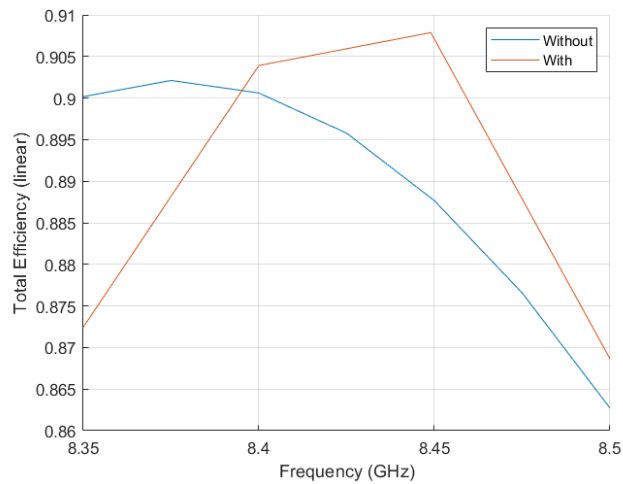


Figure 4.18-Total Efficiency with and without metamaterial

The diagrams of radiation (figure 4.19), both with a cut of 0° and 90° also didn't change a lot comparing to the array without metamaterial which is desirable.

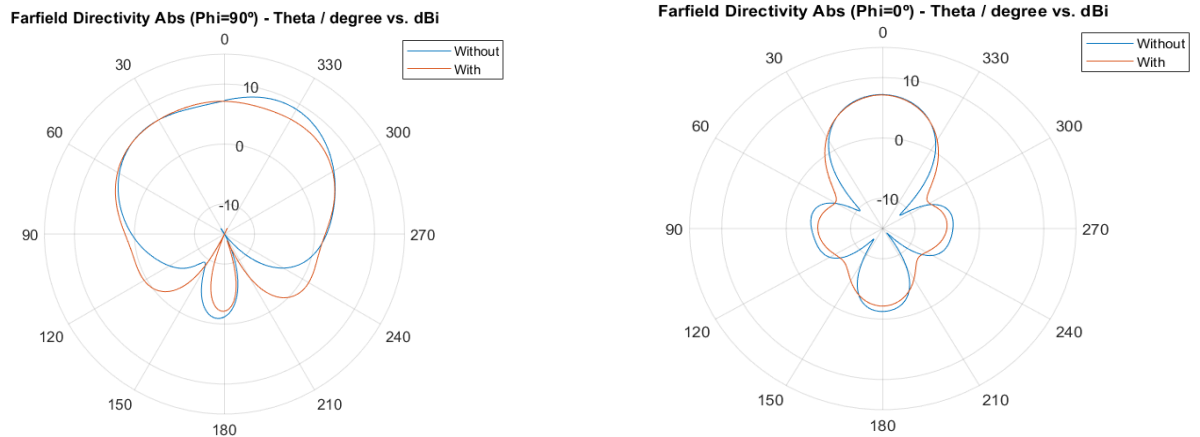


Figure 4.19-Diagrams of radiation with and without the metamaterial

In relation to the Diversity gain and ECC (figure 4.20), although the results are almost the same, with the double ring metamaterial the results are not as good as the previous metamaterial.

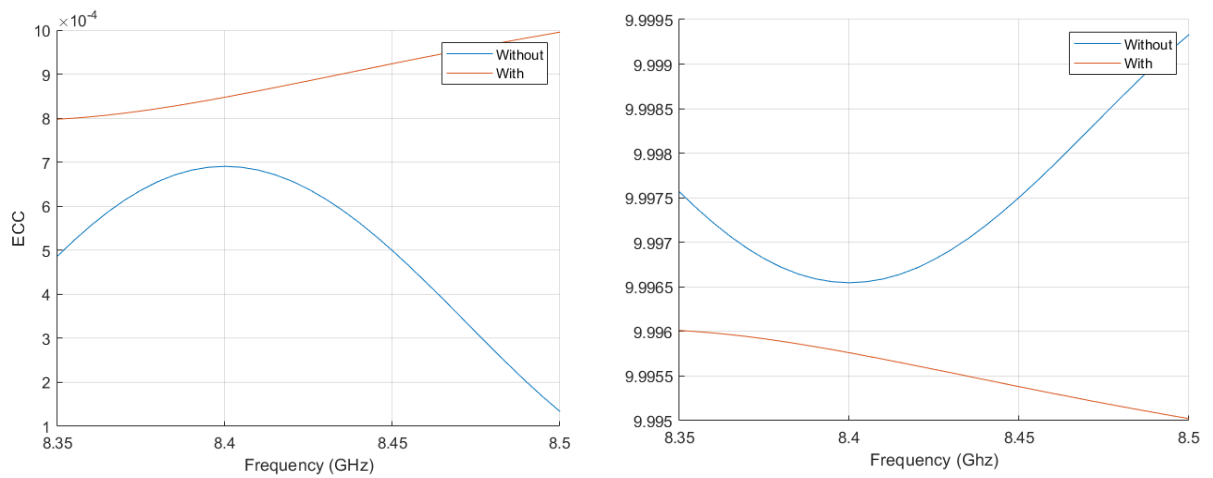


Figure 4.20-ECC and Diversity Gain with and without metamaterial

4.2.3 U Shape metamaterial in an array with recessed feed

After analysing the effects of the metamaterials on the antenna arrays with the coaxial feed, it was also done an experiment where the feed of the antennas was done by the recessed method instead of the coaxial.

It's important to understand that the best method of alimentation to use when implementing the metamaterial is with the coaxial feed, because in cases where the array

gets a lot of elements, it needs to be space between them to put the metamaterial, and the recessed feed could disturb that.

Despite of that, it also was analysed one case where feed was the recessed to have the reference that with other methods of alimentation, the periodic structure would work the same way.

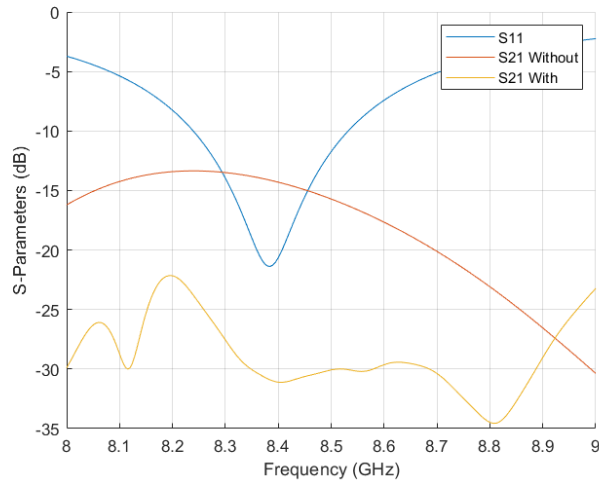


Figure 4.21-S21 with and without metamaterial

Once more it's possible to conclude that although the type of alimentation has changed, there is still a good reduction of the coupling at the resonant frequency (figure 4.21). The resonant frequency (S11) of the antenna array presented on the figure 4.21 happens when there isn't metamaterials on the structure.

The other parameters will not be analysed here, hence the outcome of the experiment presented a similar effect to the one presented on the **4.2.1 section**.

5. Prototypes and measured results

This chapter describes the manufacture, methods, and result analysis of the antenna arrays with four elements

5.1 Design and comparison of the coupling

Although both of the two metamaterials presented previously had good performances when they were placed in the antenna array, the U shape metamaterial had better results, so, to better test it's usability, the U shape metamaterial will be used to reduce the coupling of an antenna array of 4 elements.

When this periodic structure was being adapted to the antenna array of 4 elements, it had to be sure that the design and the position of the antennas as well as the position of the metamaterial was made in such a way that the surface currents were reduced, because contrarily to the antenna array with 2 elements, some things that might seemed obvious at a first glance, could have a big influence on the flow of the surface currents making the effect of the metamaterial virtually null.

For example, it had to be taken into account the feed position of all elements (in which the two of the bottom were placed symmetrically compared to the ones of the top).

Also, the thickness of the substrate needs to have a certain value, so one of the predominant sources of coupling on the array came from the surface currents, to achieve a good outcome (indeed, this one was not so critical as at frequencies at around 8.4GHz, the substrate doesn't have an outstanding impact on the array, but at higher frequencies it could start to have an influence).

Furthermore, The CSRR was placed on both sides of the structure to give a better isolation (top of the substrate and ground) as with the metamaterial only on the top of the substrate the reduction was not so great as with two elements.

In order to observe the different values of coupling between the two antenna arrays it was initially compared the results of the simulation.

As the results were extremely similar between all the elements due to its symmetry, it will only be analysed the case of the coupling of antenna number one compared to the other elements.

The following image provides numbers that were addressed to each one of the antennas (figure 5.1).

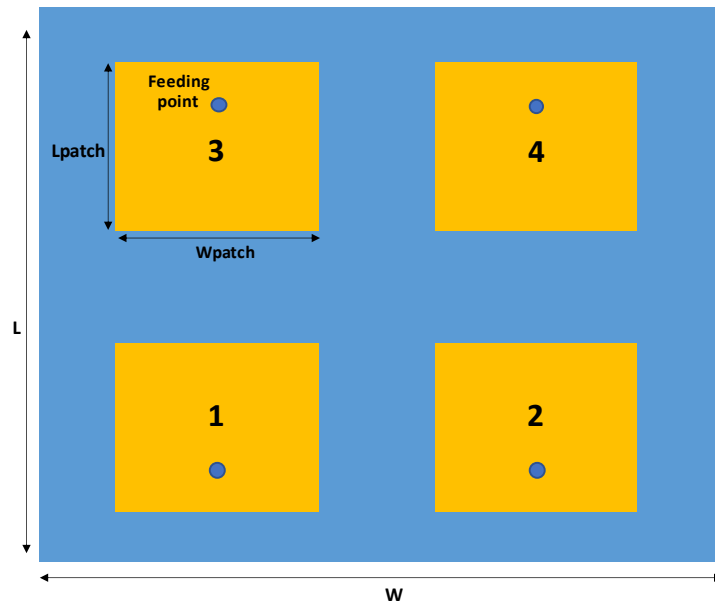


Figure 5.1-Numbering of the antenna elements.

Observing the figure 5.2, it's possible to see that the reflection coefficient of the antenna 1 in both cases is well adapted. However, with the periodic structure the is even better.

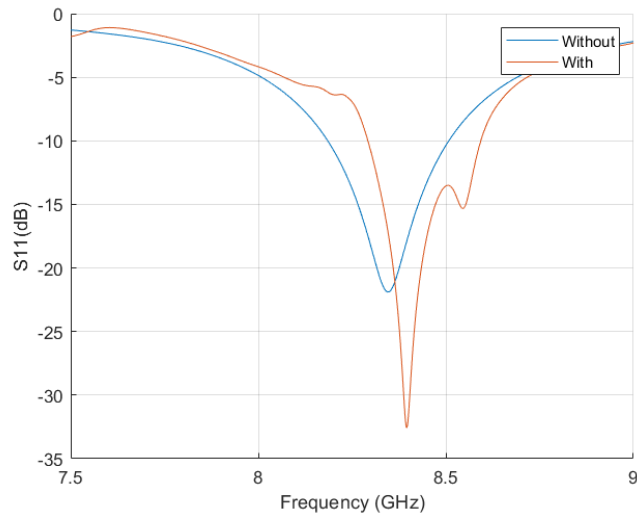


Figure 5.2-S11 with and without metamaterial

The slightly shift on the frequency of the antenna 1 when the array has the periodic structure is normal and occurs due to the proximity of the antenna with the metamaterials,

which produces a slow-wave effect on the array and slightly changes the impedance matching. [19]

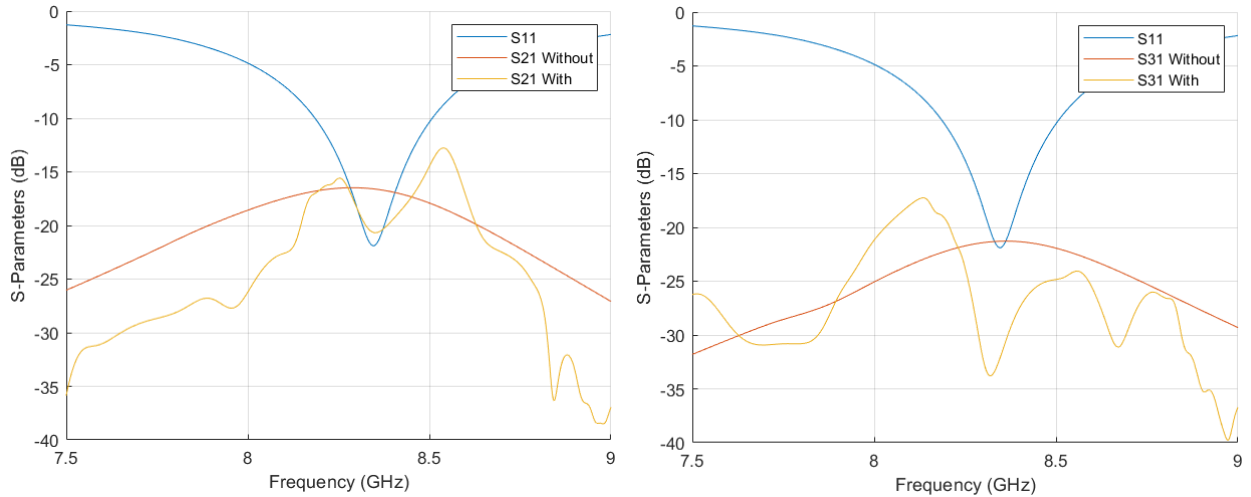


Figure 5.3-S21 and S31 with and without metamaterial

When the periodic metamaterial structure is inserted on the structure both the coupling in E-plane and H-plane are reduced as it's possible to observe on the figure 5.3. The coupling between the antenna 1 and antenna 2 decreases by approximately 4dB at the resonant frequency, and the coupling between the antenna 1 and antenna 2 decreases by 12dB.

This transpose of the S21 and S31 makes up an important change on the coupling, because without the periodic structure both values are less than 30dB which constitutes a negative impact on the antenna array, and although the S21 didn't went to less than 30dB, it was still an important decrease as the power lost decreases from 0.022mW to 0.0089mW.

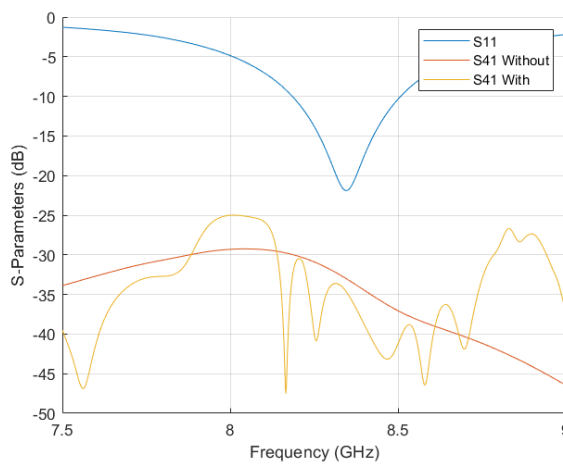


Figure 5.4-S41 with and without metamaterial

In regard to the coupling of the antennas on the diagonal, this is, the antenna 1 and antenna 4, there is also a decrease in the coupling (figure 5.4), however, this one was already low (around -30dB and below) without the metamaterials because the antennas were too far apart.

After seeing that the coupling of the elements was reduced in the simulation, both antenna arrays were printed and manufactured to compare the results in a real situation.

On the following image (figure 5.5) it's possible to see the prototypes of the two array antenna that were tested: On the left, the array without the metamaterial, and on the right, the array with the periodic structure embedded on it.

The CSRR was placed on both sides of the structure to give a better isolation.[19]

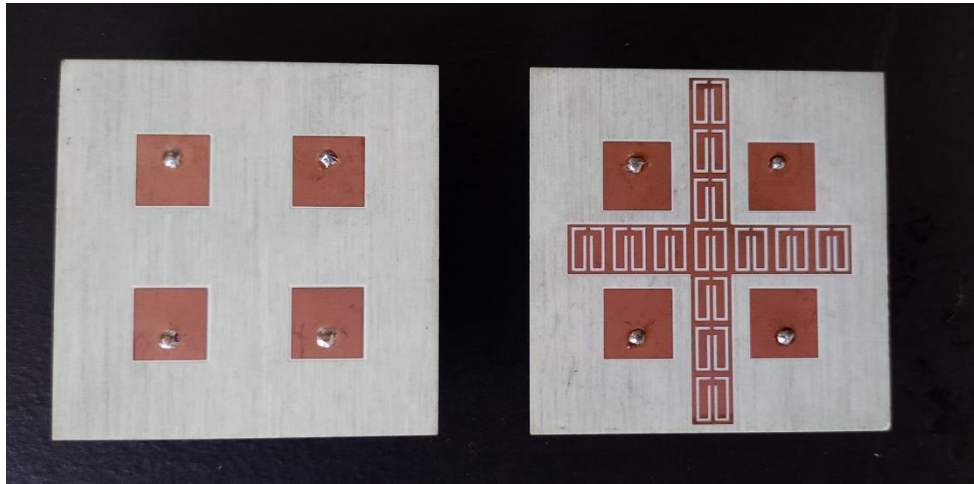


Figure 5.5-Metamaterial prototypes fabricated

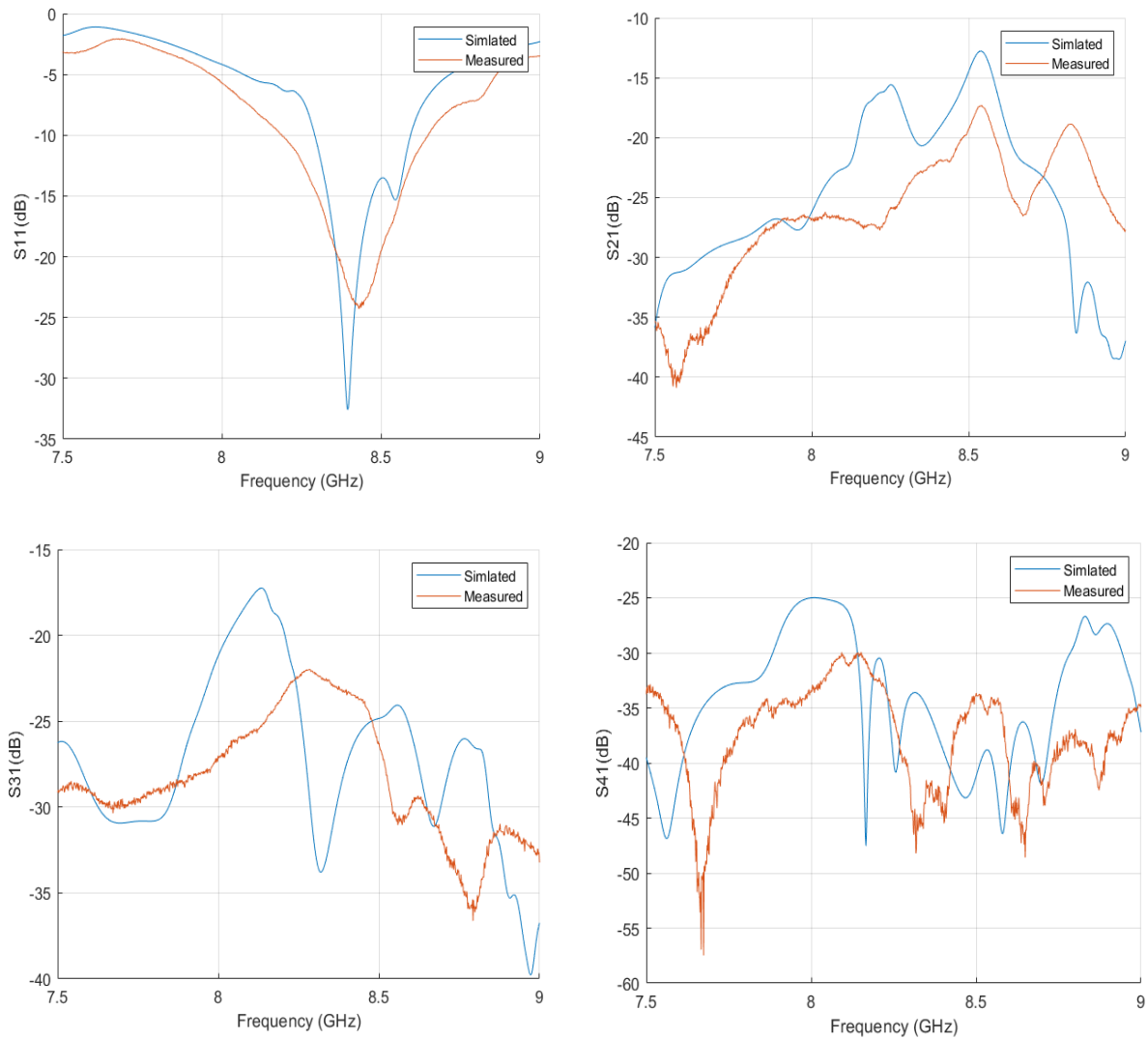


Figure 5.6-S11, S21, S31 and S41 simulated and measured with metamaterial

Firstly, it was compared the results with the metamaterial in simulation and in real life to see if there wasn't any big difference.

Seeing the graphs of the figure 5.6 it's possible to see that on the measured results, all the values had a similar wave shape and values, however in the measured results, there as a slightly shift of the wave, especially on the coupling graphs.

This is easily explained because the printer wasn't 100% precise on the dimensions, and in the metamaterial, a minor change on the dimensions can cause a significant shift on its frequency of adaptation, so although there was a slight shift in the frequency, this was not critical, and the reduction could be easily compared at around 8.65GHz instead of 8.4GHz.

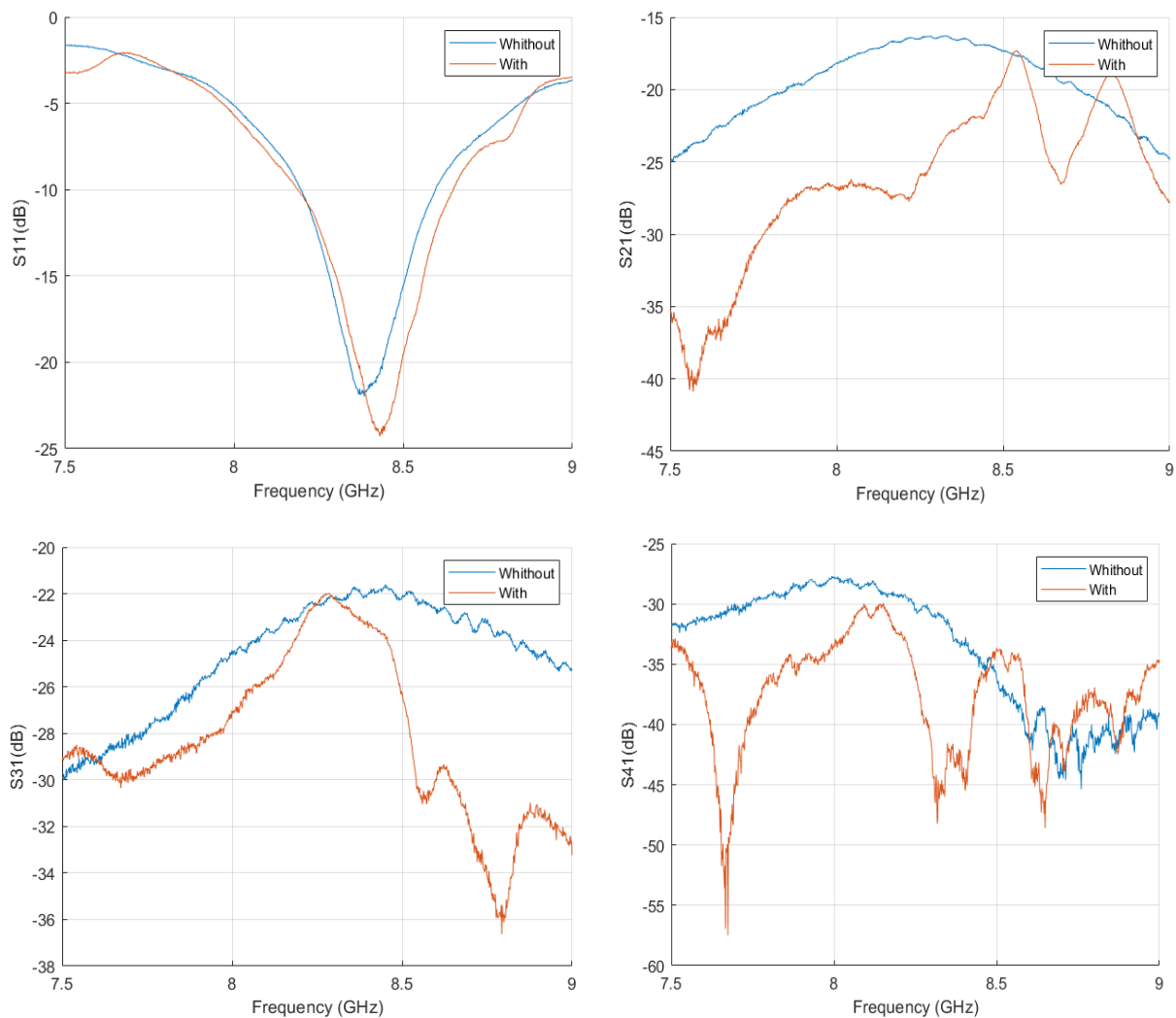


Figure 5.7-S11, S21, S31 and S41 measured with and without metamaterial

Comparing the graphs of the measured results with and without metamaterial (figure 5.7), and despite the slightly shift of the frequency, it can be seen that the final results tend to be similar to the ones simulated, as it was expected.

Although at 8.4GHz there isn't a significant difference, at the frequency where the metamaterial provides the minimum value of coupling, it's possible to see that the S21 decreased 6dB and the S31 decreased 11dB, which is very similar to the simulated results.

Despite the fact that the S41 increased a little bit near the frequencies where the E-plane and H-plane had its minimums, it's despicable because the value is nearly -40dB which is very low.

The table below shows a more specific overview of the values of the coupling and reinforces the fact that the resonant frequency of the antennas should be synchronized with the frequency where the metamaterial provides its minimum (that's the frequency that the surface currents are cancelled the best) because, even though there were good improvements at 8.4GHz on the measured results, they could be better if there was that synchronization.

5.2 Comparison of other parameters apart from coupling

Simulated results (@ 8.4GHz)	W/O Metamaterial	W/ Metamaterial	Effect
S11	-22dB	-18dB and -33dB at 8.45GHz	A 50 MHz shift on the adaptation frequency
S21	-17dB	-21dB	-4dB
S31	-21dB	-33dB	-12dB
S41	-33dB	-35dB	-3dB (but it was already low)
Measured results (@ 8.4GHz)	W/O Metamaterial	W/ Metamaterial	Effect
S11	-22dB	-22dB and -24dB at 8.45GHz	A 50 MHz shift on the adaptation frequency
S21	-16dB	-23dB	-6dB
S31	-22dB	-23dB	-1dB
S41	-33dB	-45dB	-12dB (but it was already low)
Measured results (@ 8.65GHz)	W/O Metamaterial	W/ Metamaterial	Effect
S21	-20dB	-26dB	-6dB
S31	-23dB	-34dB	-11dB
S41	-40dB	-40dB	No significant changes, and its low.

Table 5.1-Simulated and measured values of the antenna array with and without metamaterial

After analysing the coupling and concluding that with the metamaterial there is a reduction of it, it's also important to consider other parameters too see if there is not a big trade off of the array performance.

Firstly, it was analysed the total efficiency (figure 5.8) and it's possible to see that there is a small reduction (about 5%) on the frequency of adaptation due to dielectric losses, however it is still high.

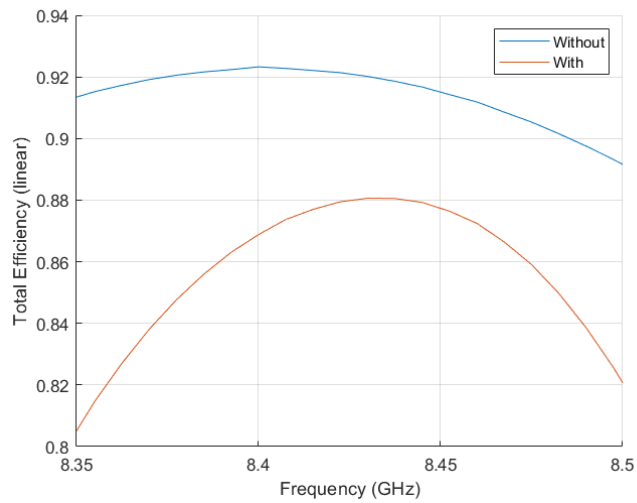


Figure 5.8-Total Efficiency with and without metamaterial

In regard to the value of the realized gain, it didn't have a lot of changes at 8.4GHz as it's possible to see in the figure 5.9. There is a little bit of increase at the adaptation frequency and a little bit of decrease near that area.

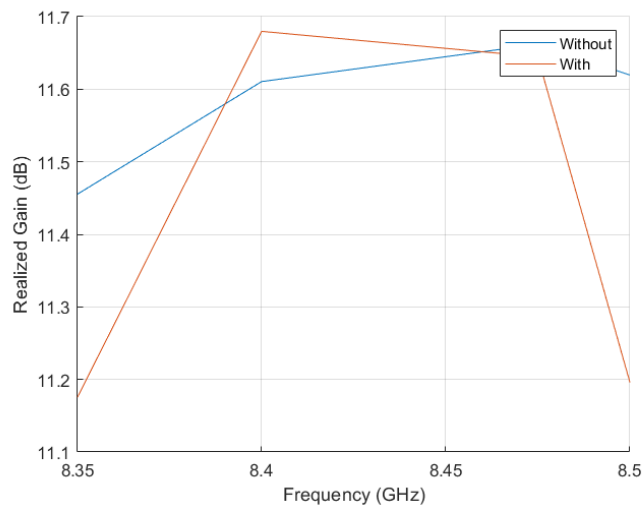


Figure 5.9-Realized Gain with and without metamaterial

The ECC and Diversity Gain had some improvements at 8.4GHz as it was expected in spite of this values were already good without the metamaterial.

By the figure 5.10, it can be concluded that the ECC hits values near to zero which is the ideal, and in consequence of that the DG has a higher value.

With these values of ECC and DG, it can be concluded that the metamaterial provides a good safety against diagram radiation degradation, which is a strong characteristic to look for in structures to reduce coupling.

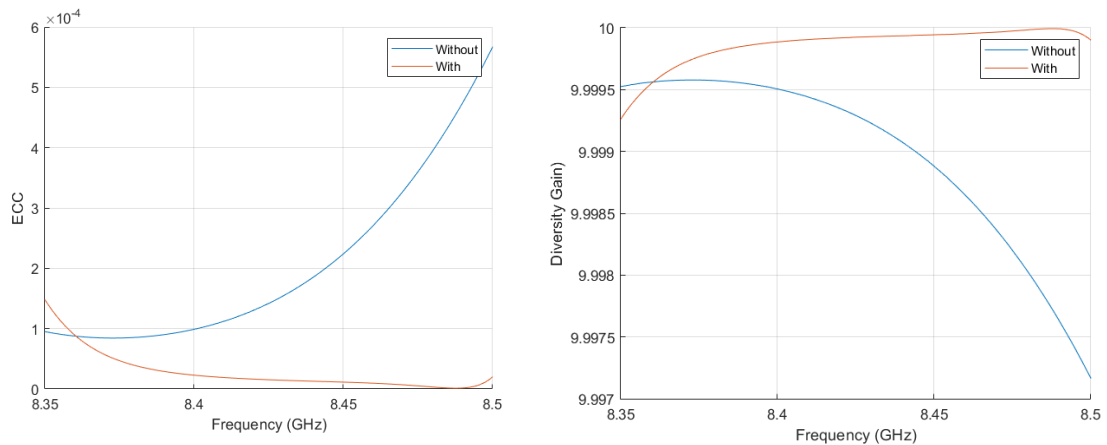


Figure 5.10-ECC and Diversity Gain with and without metamaterial

To finish the analysis, it's possible to see that with the metamaterial, the simulated diagrams of radiation (figure 5.11) with a cut angle of 90° and 0° didn't suffer a significant alteration comparing without the metamaterial, which is ideal as the less it changes (when the diagrams of the array without the metamaterials are not degraded), the better.

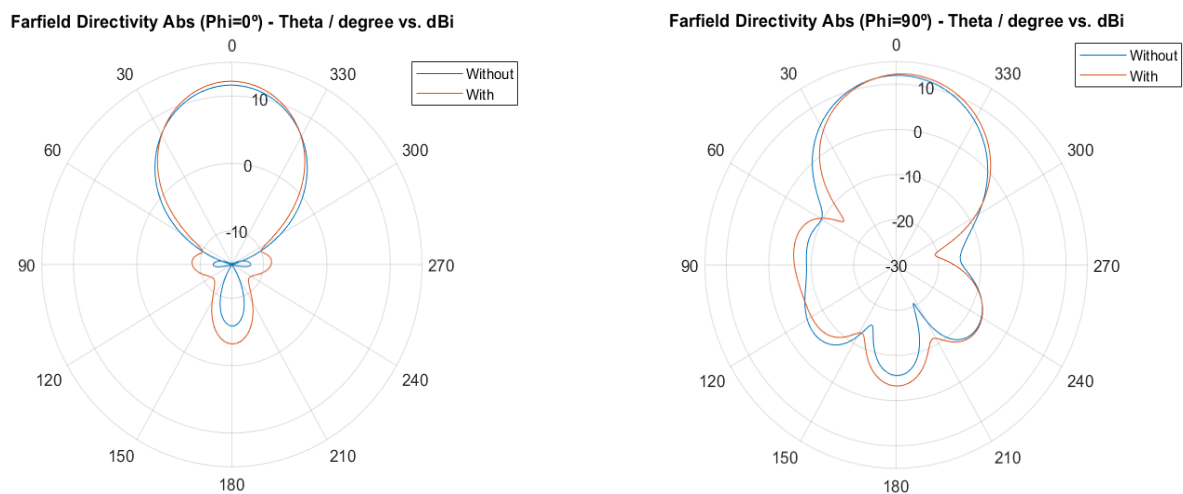


Figure 5.11-Diagrams of radiation with and without the metamaterial

With that said, it can be concluded that with the metamaterial, the coupling between antennas in an array MIMO can be reduced, without losing a significant performance of it, as long as the minimum of the metamaterial is overlapping the resonant frequency of the antennas of the MIMO array.

6. Conclusions and future work

This chapter presents the conclusions of the work developed and suggestions for future work.

6.1 Conclusions

The principal objective of this dissertation was to design, develop and test a technique that allow the MC reduction between elements of an antenna array. During this work, several aspects were considered to produce the best technique possible.

Initially, it was considered several techniques and perspectives that were previously studied and developed in order to understand what was the best one, to give the best possible launch pad, and, from the best path, it was also studied his fundamentals to extract as much crucial information as possible to achieve the best outcome. From this, two metamaterials were developed and simulated under different sets of arrays.

Finally, the best one was fabricated and tested, achieving a good result when compared to the results of the simulated version.

The more challenging tasks were trying to achieve similar results on the fabricated prototype compared to the simulated ones, as there have been developed other prototypes that worked well on the simulation but weren't as convincing on the real tests. Furthermore, when implementing the array of four elements, it had to be considered variables that as first glance seemed to be obvious but could have influence on the flow of the surface currents making the effect of the periodic structure not be the desirable.

Even though there were some adversities during the development of the arrays, and on the final result were slightly deviations on the frequency, overall, these results were successful, and the primary goal of this dissertation was achieved.

Concluding, the metamaterials presented have potential to reduce the coupling on the current antenna arrays around the frequency studied.

6.2 Future work

To further improve this work, these suggestions are made to enhance the results obtained:

- Insert and test the metamaterials in bigger arrays.

- Test the periodic structures for arrays in higher frequencies.
- Study the symmetry and the positions of the elements of the array and the metamaterials in order to have a better cancellation of the surface currents.
- Analyse the effect of the metamaterial on thinner substrates.

References

- [1] "how-5g-massive-mimo-transforms-your-mobile-experiences @ www.qualcomm.com." [Online]. Available: <https://www.qualcomm.com/news/onq/2019/06/how-5g-massive-mimo-transforms-your-mobile-experiences>
- [2] "What-is-Beamforming-Beam-steering-and-Beam-switching-with-Massive-MIMO @ www.metaswitch.com." [Online]. Available: <https://www.metaswitch.com/knowledge-center/reference/what-is-beamforming-beam-steering-and-beam-switching-with-massive-mimo>
- [3] J. Bernardo and S. Caiado, "Wideband antenna arrays for mmWaves.", 2019. doi: <http://hdl.handle.net/10773/29791>
- [4] Inc. 9710 C. Ave. C. C. 91311 A.H Systems, "Practical overview of antenna parameters."
- [5] A. Iqbal, O. A. Saraereh, A. Bouazizi, and A. Basir, "Metamaterial-based highly isolated MIMO antenna for portable wireless applications," *Electronics (Switzerland)*, vol. 7, no. 10, Oct. 2018, doi: 10.3390/electronics7100267.
- [6] "Diversity gain," Jan. 29, 2021. https://en.wikipedia.org/wiki/Diversity_gain (accessed Jun. 05, 2022).
- [7] Balanis, C. *Balanis, Teoria das antenas, Volume 1-Rio de Janeiro: LTC,2009.* translation of Antenna theory: analysis and design, 3rd ed (2005). ISBN: 978-85-216-1653-5
- [8] H. S. Lui, H. T. Hui, and M. S. Leong, "A note on the mutual-coupling problems in transmitting and receiving antenna arrays," *IEEE Antennas Propag Mag*, vol. 51, no. 5, pp. 171–176, 2009, doi: 10.1109/MAP.2009.5432083.
- [9] Balanis, C. A. *Balanis, Antenna Theory: Analysis and Design. USA: Wiley-Interscience, 2017, isbn: 978-1-118- 64206-1.*
- [10] M. I. Ahmed, A. Sebak, E. A. Abdallah, and H. Elhennawy, "Mutual coupling reduction using defected ground structure (DGS) for array applications," *2012 15th International Symposium on Antenna Technology and Applied Electromagnetics, ANTEM 2012*, pp. 25–29, 2012, doi: 10.1109/ANTEM.2012.6262354.
- [11] M. Harbel, J. Zbitou, M. Hefnawi, and M. Latrach, "Mutual Coupling Reduction in MmWave Patch Antenna Arrays Using Mushroom-like EBG Structure," in *2020 IEEE 2nd International Conference on Electronics, Control, Optimization and Computer Science, ICECOCS 2020*, Dec. 2020. doi: 10.1109/ICECOCS50124.2020.9314440.
- [12] Z. Qamar and H. C. Park, "Compact waveguided metamaterials for suppression of mutual coupling in microstrip array," *Progress in Electromagnetics Research*, vol. 149, no. January 2014, pp. 183–192, 2014, doi: 10.2528/PIER14063002.

- [13] G. Donzelli, F. Capolino, S. Boscolo, and M. Midrio, "Elimination of scan blindness in phased array antennas using a grounded-dielectric EBG material," *IEEE Antennas Wirel Propag Lett*, vol. 6, pp. 106–109, 2007, doi: 10.1109/LAWP.2007.892043.
- [14] J. R. Rao, P. Zong, and D. R. Becerra, "Mutual coupling effect of microstrip antenna array," in *Procedia Engineering*, 2012, vol. 29, pp. 1984–1988. doi: 10.1016/j.proeng.2012.01.248.
- [15] G. Donzelli, F. Capolino, S. Boscolo, and M. Midrio, "Elimination of scan blindness in phased array antennas using a grounded-dielectric EBG material," *IEEE Antennas Wirel Propag Lett*, vol. 6, pp. 106–109, 2007, doi: 10.1109/LAWP.2007.892043.
- [16] J. Ghosh, S. Ghosal, D. Mitra, and S. R. B. Chaudhuri, "Mutual coupling reduction between closely placed microstrip patch antenna using meander line resonator," *Progress in Electromagnetics Research Letters*, vol. 59, no. March, pp. 115–122, 2016, doi: 10.2528/PIERL16012202.
- [17] J. Ghosh, S. Ghosal, D. Mitra, and S. R. B. Chaudhuri, "Mutual coupling reduction between closely placed microstrip patch antenna using meander line resonator," *Progress in Electromagnetics Research Letters*, vol. 59, no. March, pp. 115–122, 2016, doi: 10.2528/PIERL16012202.
- [18] M. F. Shafique, Z. Qamar, L. Riaz, R. Saleem, and S. A. Khan, "Coupling suppression in densely packed microstrip arrays using metamaterial structure," *Microw Opt Technol Lett*, vol. 57, no. 3, pp. 759–763, Mar. 2015, doi: 10.1002/mop.28943.
- [19] Z. Qamar and H. C. Park, "Compact waveguided metamaterials for suppression of mutual coupling in microstrip array," *Progress in Electromagnetics Research*, vol. 149, no. January 2014, pp. 183–192, 2014, doi: 10.2528/PIER14063002.
- [20] H. X. Xu, G. M. Wang, and M. Q. Qi, "Hilbert-shaped magnetic waveguided metamaterials for electromagnetic coupling reduction of microstrip antenna array," *IEEE Trans Magn*, vol. 49, no. 4, pp. 1526–1529, 2013, doi: 10.1109/TMAG.2012.2230272.
- [21] S. Farsi, H. Aliakbarian, D. Schreurs, B. Nauwelaers, and G. A. E. Vandenbosch, "Mutual coupling reduction between planar antennas by using a simple microstrip U-section," *IEEE Antennas Wirel Propag Lett*, vol. 11, pp. 1501–1503, 2012, doi: 10.1109/LAWP.2012.2232274.
- [22] M. E. T. U. Prof. Gönül Turhan-Sayan, "'Metamaterial Research with Applications in Microwave, Terahertz and Infrared Bands'-IEEE AP/MTT/EMC/ED Turkey Seminars - Prof. Gönül Turhan Sayan, December 22, 2017." https://www.youtube.com/watch?v=Y0yH_L-uG4I&t=926s (accessed Jun. 04, 2022).
- [23] skullsinthestars, "Some musings on negative refraction," Jul. 04, 2009. <https://skullsinthestars.com/2009/07/04/some-musings-on-negative-refraction/> (accessed Jun. 05, 2022).
- [24] M. Johri and H. Paudyal, "LEFT HANDED MATERIALS: A NEW PARADIGM IN STRUCTURED ELECTROMAGNETICS Seismic Hazard in Asia View project Dielectric property View project," 2010. [Online]. Available: <https://www.researchgate.net/publication/260087087>

- [25] M. Pinheiro and S. Neto, "UNIVERSIDADE FEDERAL DO RIO GRANDE DO NORTE CENTRO DE TECNOLOGIA PROGRAMA DE PÓS-GRADUAÇÃO EM ENGENHARIA ELÉTRICA E DE COMPUTAÇÃO Um Estudo de Metamaterial em Antenas de Microfita."
- [26] L. Solymar and E. Shamonina, "Waves in Metamaterials." 2009. Published in the United States by Oxford University Press Inc., New York. ISBN: 978-0-19-921533-1
- [27] J. D. Baena *et al.*, "Equivalent-circuit models for split-ring resonators and complementary split-ring resonators coupled to planar transmission lines," *IEEE Trans Microw Theory Tech*, vol. 53, no. 4 II, pp. 1451-1460, Apr. 2005, doi: 10.1109/TMTT.2005.845211.
- [28] ANSYS, "Getting Started with HFSS™ Floquet Ports," 2015. [Online]. Available: <http://www.ansys.com>